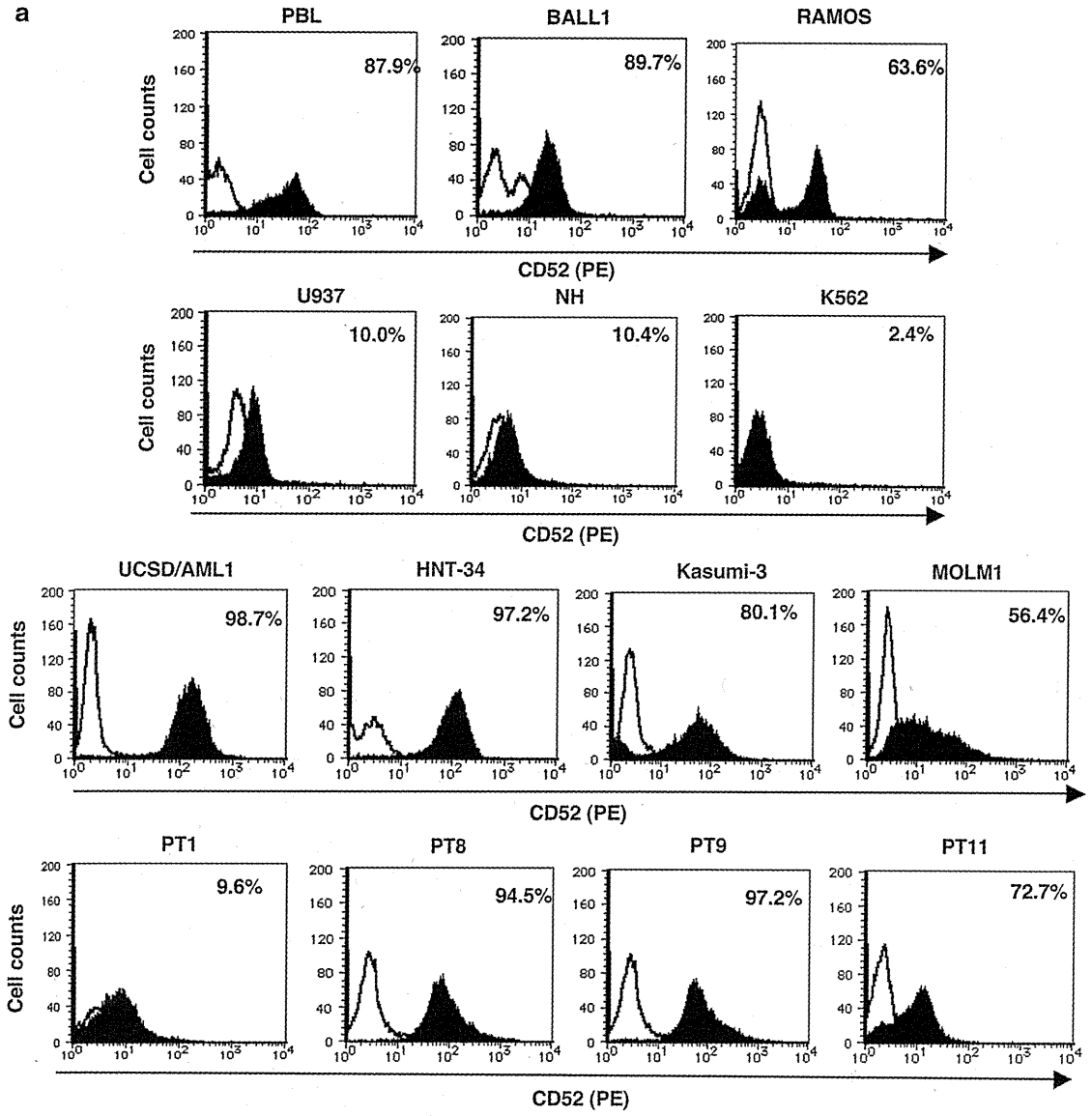
a
PBL
87.9%
BALL1
89.7%
RAMOS
63.6%
U937
10.0%
NH
10.4%
K562
2.4%
UCSD/AML1
98.7%
HNT-34
97.2%
Kasumi-3
80.1%
MOLM1
56.4%
PT1
9.6%
PT8
94.5%
PT9
97.2%
PT11
72.7%
Cell counts
CD52 (PE)
b
U937
Parental
Mock
EVI1
EVI1
CD52
β-actin
c
U937/Mock
U937/EVI1
Cell counts
CD52(PE)
d
UCSD/AML1
Parental
shLuc
shEVI1
EVI1
CD52
β-actin
e
AML1/shEVI1
AML1/shLuc
Cell counts
CD52(PE)

A microarray analysis of the samples from the EVI1^{High} AML cells versus the EVI1^{Low} AML cells confirmed upregulation of CD52 in the EVI1^{High} AML cells (Supplementary Figure S1). Because a humanized anti-CD52 antibody, CAMPATH-1H, has already been developed for immunosuppression before bone marrow transplantation and for gene-targeted therapy for

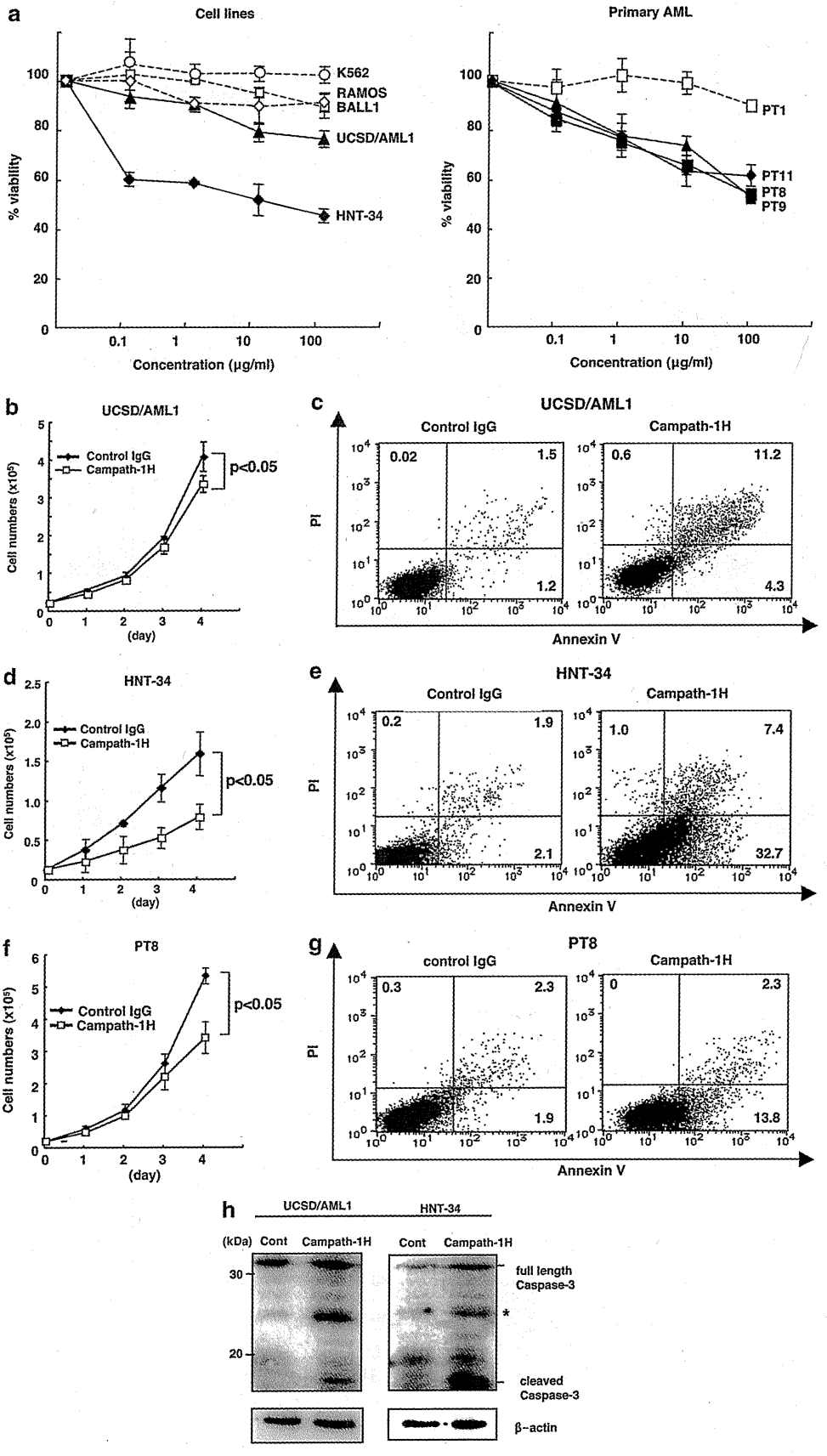

lymphoproliferative disorders, we further analyzed whether the CD52 antigen is a novel target in EVI1^{High} AML.

In the next experiment, CD52 expression was examined in 15 myeloid leukemia cell lines and primary leukemia cells from 12 patients with AML using RT-PCR. We included three additional cell lines without chromosome 3q26 abnormalities (U937, K562 and KG-1) in the analysis. The CD52 expression levels in four cell lines with EVI1^{High} expression (UCSD/AML1, HNT-34, Kasumi-3 and MOLM-1) were higher than that in the other 11 cell lines with EVI1^{Low} expression (Figure 1b, top). In primary leukemia cells, EVI1 and CD52 were more highly expressed in nine patients with chromosome 3q26 abnormalities than that in three patients without chromosome 3q26 abnormalities (Figure 1b, bottom). Thus, CD52 may be a potential marker for EVI1^{High} myeloid leukemia cells.

CAMPATH-1H identifies the CD52 antigen on the surface of EVI1^{High} myeloid leukemia cells

Next, we determined the surface expression of the CD52 antigen by FACS analysis using phycoerythrin-labeled CAMPATH-1H (Figure 2a). We used control PB lymphocytes from a healthy volunteer and two B lymphoid leukemia cell lines (BALL1 and RAMOS) as positive controls and 63.6–89.7% of these cells were labeled by CAMPATH-1H. In EVI1^{Low} myeloid leukemia cell lines (U937, NH and K562) and primary AML cells from a patient with EVI1^{Low} (PT1), 2.4–10.4% of the cells were labeled by CAMPATH-1H with a low signal intensity. In contrast, 56.4–98.7% of EVI1^{High} myeloid leukemic cells (UCSD/AML1, HNT-34, Kasumi-3 and MOLM1) were robustly labeled by CAMPATH-1H, yielding higher signal intensity than BALL1 and RAMOS cells. Moreover, CAMPATH-1H bound to the majority of leukemia cells from three AML patients with inv(3)(q21q26) (PT8 and PT9) or with t(3;21)(q26;q22) (PT11) at a high signal intensity similar to EVI1^{High} cell lines.

To determine whether the EVI1 transcription factor activates CD52 gene expression, we introduced an EVI1 expression vector into an EVI1^{Low} leukemia cell line, U937, and an shRNA targeting EVI1 (shEVI1) into an EVI1^{High} leukemia cell line, UCSD/AML1. After introducing the EVI1 expression vector into U937 cells, the expression of EVI1 was clearly detected in U937/EVI1 cells by RT-PCR, and the level of CD52 mRNA was also increased in U937/EVI1 cells in comparison with parental or mock vector-transfected cells (Figure 2b). FACS analysis showed that the population of CD52-positive cells was increased (61.1%) in U937/EVI1 cells in comparison to U937/mock cells (19.3%), with increased fluorescence intensity (Figure 2c). Moreover, after the introduction of shEVI1 or shRNA against luciferase (shLuc) as a control into UCSD/AML1 cells, the expression level of CD52 mRNA was decreased in UCSD/AML1/shEVI1 cells, along with a decreased expression of EVI1, when compared with parental or UCSD/AML1/shLuc cells (Figure 2d). FACS analysis showed that the percentage of CD52-positive cells in AML1/shEVI1 cells was considerably lower (24.0%) than that in AML1/shLuc (45.1%) cells with decreased fluorescence (Figure 2e). Thus, the CD52 expression in myeloid leukemic cells is partly dependent on the expression of EVI1, and CD52 may be one of the downstream target genes regulated directly or indirectly by EVI1.

CAMPATH-1H induced a direct cytotoxic effect on EVI1^{High} AML cells

Because CAMPATH-1H was highly reactive with the surface of EVI1^{High} AML cells, it may be a good therapeutic candidate for EVI1-positive AML. We initially tested the growth inhibitory and direct cytotoxic effects of CAMPATH-1H on an EVI1^{Low} AML cell line (K562) and two EVI1^{High} AML cell lines (UCSD/AML1 and HNT-34) with two B-ALL cell lines (BALL1 and RAMOS) as controls. After the cells were incubated with various concentrations of CAMPATH-1H for 48 h, the cell viability was evaluated by Trypan blue staining (Figure 3a). Cell growth was inhibited in the three AML cell lines with EVI1^{High} expression in a dose-dependent manner, and 51.5–78.9% of cells remained viable at 10 μg/ml CAMPATH-1H. In contrast, over 90% of B-ALL cells were viable at this drug concentration. In the next experiment, primary AML cells from a patient with EVI1^{Low} expression (PT1) and from three patients with EVI1^{High} expression (PT8, PT9 and PT11) were used to test the direct cytotoxic effect of CAMPATH-1H. Over 90% of PT1 cells were viable at all drug concentrations; however, only 52.5–57.5% of EVI1^{High} AML cells from patients (PT8, PT9 and PT11) survived the maximal dose of 100 μg/ml, suggesting that CAMPATH-1H directly suppressed the survival of EVI1^{High} AML cells.

To confirm whether the cytotoxic effect of CAMPATH-1H is dependent on apoptotic cell death, we treated two EVI1^{High} AML cell lines (UCSD/AML1 and HNT-34) and primary EVI1^{High} AML cells (PT8) with 10 μg/ml of CAMPATH-1H for 4 days and determined the cell viability and apoptosis. In all of the EVI1^{High} AML cells, the growth rate of CAMPATH-1H-treated cells was slower than that of control immunoglobulin G (IgG)-treated cells (Figures 3b, d and f) and 15.5–40.1% of EVI1^{High} AML cells underwent apoptosis 2 days after treatment (Figures 3c, d and f). Moreover, the amount of cleaved caspase-3 (18 kDa) was increased in the EVI1^{High} leukemic cells after 2 days of CAMPATH-1H treatment (Figure 3h). Thus, our results indicate that CAMPATH-1H effectively induces apoptosis in EVI1^{High} AML cells.

CAMPATH-1H-mediated CDC and ADCC against EVI1^{High} AML cells

Because CAMPATH-1H exerts its antitumor effects on lymphocytes or lymphoid leukemia cells through immunological mechanisms, such as CDC and/or ADCC, by virtue of its

Figure 3 Induction of direct cytotoxicity against EVI1^{High} AML cells by CAMPATH-1H treatment. (**a**) Viable cells after treatment with the indicated concentration of CAMPATH-1H for 48 h were examined using Trypan blue dye exclusion and are shown as the percentages of the values obtained from the untreated parental cells. The left panel shows the percent viability of cell lines with EVI1^{Low} expression (K562, RAMOS and BALL1; dot lines with open marks) and with EVI1^{High} expression (UCSD/AML1 and HNT34; solid lines with closed marks). The right panel shows the percent viability of primary AML cells with EVI1^{Low} expression (PT1; dot lines with open marks) and with EVI1^{High} expression (PT8, PT9 and PT11; solid lines with closed marks). The experiments were performed in triplicate and repeated independently at least three times. (**b**, **d**, **f**) Viable cell numbers of EVI1^{High} AML cells (UCSD/AML1, HNT-34 and PT8) were shown at the indicated time points after treatment with 10 μg/ml of CAMPATH-1H or with control IgG. Student's *t*-test ($P<0.05$) was used for the statistical analysis between the control IgG- and CAMPATH-1H-treated AML cells. (**c**, **e**, **g**) CAMPATH-1H treatment induces the apoptosis of EVI1^{High} AML cells. Following treatment with CAMPATH-1H for 48 h, cells were labeled with Annexin-V and propidium iodide, and the percent of apoptotic cells was determined using flow cytometry. The experiments were performed in triplicate and repeated independently at least three times. (**h**) Identification of cleaved caspase-3 after the treatment with CAMPATH-1H against EVI1^{High} AML. EVI1^{High} AML cell lines (UCSD/AML1 and HNT-34) were treated with CAMPATH-1H (10 μg/ml) for 48 h, and western blot analyses were performed by anti-caspase-3 antibody. Asterisks indicate nonspecific bands.

IgG Fc region, we initially investigated the CDC activity of CAMPATH-1H on EVI1^{High} AML cell lines (UCSD/AML1 and HNT-34) along with EVI1^{Low} AML (K562) and B-ALL cell lines (BALL1 and RAMOS) as controls. CAMPATH-1H treatment induced a slight increase in cell death in the two B-ALL and two EVI1^{High} AML cell lines, although it had no effect on the EVI1^{Low} K562 cell line (Figure 4a, left panel). Next, primary AML cells from a patient with EVI1^{Low} (PT1) and from three patients with EVI1^{High} expression (PT8, PT9 and PT11) were used to test the effect of CAMPATH-1H on CDC. Only a low level of cell death was observed in the PT1 and PT8 cells, but a moderate CDC effect was observed using the PT-9 and PT11 cells (Figure 4a, right panel). Thus, CAMPATH-1H does not appear to have a significant CDC effect on EVI1^{High} AML cells.

Next, the ADCC activity of CAMPATH-1H was examined against the same cell lines and primary AML cells as those in the CDC. In the two B-ALL and two EVI1^{High} leukemia cell lines, CAMPATH-1H significantly increased the percentages of cell death in a dose-dependent manner, whereas EVI1^{Low} K562 cells showed almost no response (Figure 4b, left panel). Treatment

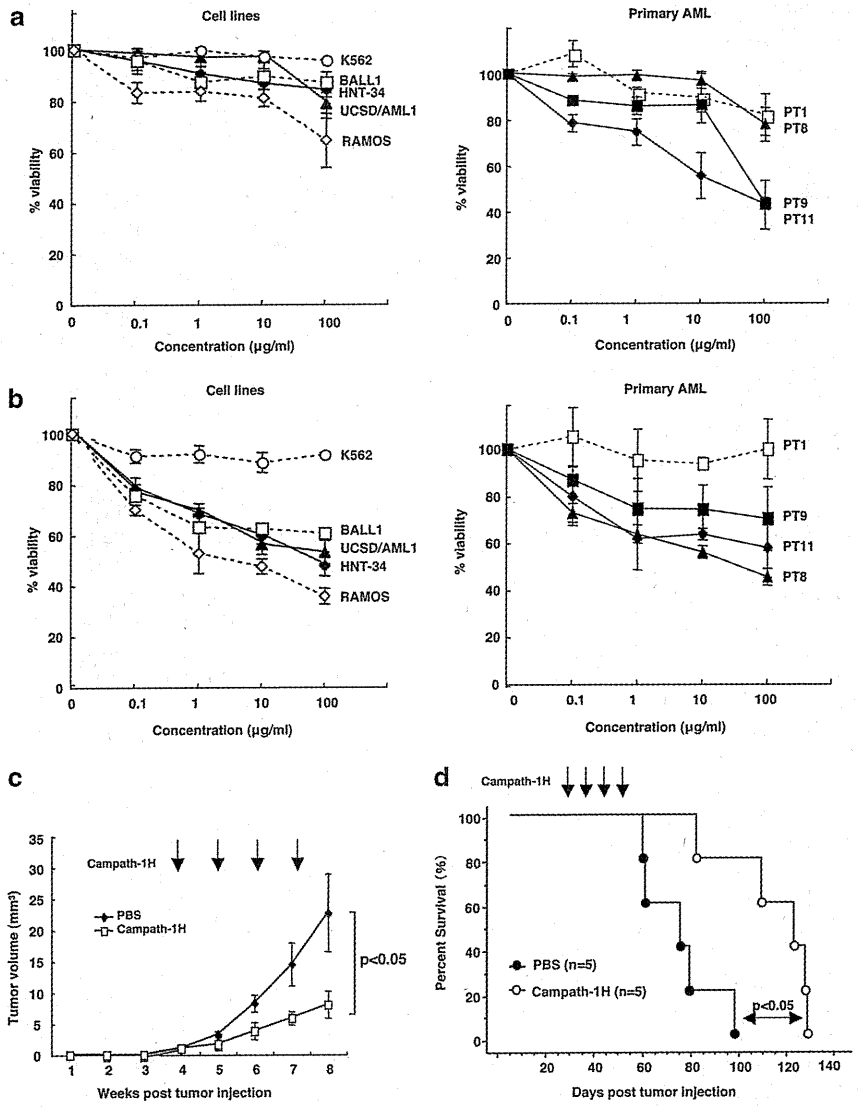

Figure 4 The induction of CDC and ADCC activities by the treatment of CAMPATH-1H and *in vivo* antitumor activity against EVI1^{High} AML cells in mouse xenograft models. (**a**) CAMPATH-1H-mediated CDC activity in various leukemia cells. The left panel shows the percent viability of cell lines with EVI1^{Low} expression (K562, RAMOS and BALL1; dot lines with open marks) and cell lines with EVI1^{High} expression (UCSD/AML1 and HNT34; solid lines with closed marks). The right panel shows the percent viability of primary AML cells with EVI1^{Low} expression (PT1; dot lines with open marks) and AML cells with EVI1^{High} expression (PT8, PT9 and PT11; solid lines with closed marks). After the cells were incubated with human serum complement and CAMPATH-1H at concentrations from 0.1 to 100 μg/ml, the extent of cell lysis was measured with an LDH-releasing assay and is shown as the percentage of the value obtained from the untreated parental cells. The experiments were repeated independently at least three times. (**b**) CAMPATH-1H-mediated ADCC activity in various leukemia cells. ADCC assays were performed with the same series of cells used in (**a**). After incubation of the cells with PB mononuclear cells from a normal donor and 0.1–100 μg/ml of CAMPATH-1H, ADCC activity was measured by LDH release. The results are the mean and standard deviations for each sample, which was independently repeated in triplicate. (**c**) CAMPATH-1H reduces tumor growth in NOG mice xenografted with EVI1^{High} AML cells. CAMPATH-1H was administered at 4 mg/kg intravenously weekly for 4 weeks. Tumor growth was assessed by measuring the volume of each tumor at weekly intervals. Each group contained five mice. The graphs depict the average tumor volume for the PBS control group and the CAMPATH-1H-treated group ± standard error (**d**) Kaplan–Meier survival plot of UCSD/AML1-bearing NOG mice. CAMPATH-1H was administered at 4 mg/kg intravenously weekly for 4 weeks. Kaplan–Meier survival curves are shown for PBS- and CAMPATH-1H-treated groups ($n=5$ per group).

with CAMPATH-1H also resulted in a significant increase in cell death in primary cells from three patients with EVI1^{High} AML (PT8, PT9 and PT11), and no response was observed in the case of the EVI1^{Low} PT1 cells (Figure 4b, right panel). These results suggest that CAMPATH-1H exerts a significantly stronger ADCC effect than a CDC effect against EVI1^{High} AML.

In vivo *antitumor effect of CAMPATH against EVI1^{High} AML in a xenograft model*

To investigate the effects of CAMPATH-1H on EVI1^{High} AML *in vivo*, USCD/AML1 cells with EVI1^{High} expression were subcutaneously inoculated into immunodeficient NOG mice. After tumors reached a size of 50–100 mm^3, 100 μg of CAMPATH-1H or PBS as a control was intravenously injected once a week for 4 weeks, and tumor growth and mouse survival were monitored (Figures 4c and d). CAMPATH-1H significantly inhibited the tumor growth of UCSD/AML1 cells when compared with the control ($P<0.05$) (Figure 4c). The median survival time of control mice was 75 days, and all control mice died within 100 days. In contrast, the median survival was prolonged to 127 days in mice injected with CAMPATH-1H, and four out of five mice were still alive more than 100 days after inoculation. Taken together, these data suggest that CAMPATH-1H is a promising candidate therapeutic antibody for AML patients with EVI1^{High} expression.

Discussion

In this study, we found that CD52 was highly expressed in most EVI1^{High} leukemia cells. Using the humanized anti-CD52 monoclonal antibody CAMPATH-1H, we showed that CAMPATH-1H inhibited cell growth and induced apoptosis of EVI1^{High} leukemia cells through direct cytotoxicity and/or ADCC *in vitro*. Moreover, we showed the therapeutic efficacy of CAMPATH-1H in an *in vivo* model of EVI1^{High} leukemia using NOG mice. Although NOG mice lack functional T and natural killer cells, murine neutrophils were considered to be effector cells mediating ADCC as well as direct cytotoxicity in our mouse model. Indeed, CAMPATH-1H efficiently inhibited the growth of leukemia xenografts in an EVI1^{High} AML xenograft model. These data suggest that the use of CAMPATH-1H may be effective in treating myeloid leukemia with EVI1^{High}.

CD52 is a small glycosylphosphatidylinositol-linked protein of unknown function. CAMPATH-1H (Alemtuzumab), a humanized antibody against CD52, is used to deplete leukemia cells from patients with relapsed/refractory chronic lymphocytic leukemia.[15] Recent studies have suggested the effectiveness of CAMPATH-1H treatment in additional hematopoietic malignancies, including peripheral T-cell lymphoma, T-cell prolymphocytic leukemia and cutaneous T-cell lymphoma.[40–42] Although it has been reported that the majority of various subtypes of AML are negative for CD52 expression, a subset of acute myelomonocytic leukemias has been shown to exhibit CD52 expression.[13] This is consistent with our observation that a case (no. 2) out of 10 EVI1^{Low} AML cases has been diagnosed with myelomonocytic leukemia with high CD52 expression (Supplementary Figure S1). Recently, it was reported that 15 patients with CD52-positive, recurrent or refractory acute leukemia (nine patients with AML and six patients with ALL) received single-agent Alemtuzumab.[14] Interestingly, the majority of the CD52-positive AML cases had chromosome 7 abnormalities, and two cases with monosomy 7 exhibited complete remission. In our study, five of nine AML patients with EVI1^{High} expression displayed chromosomal abnormalities involving chromosome 7, such as t(3;7)(q26;q21), partial deletion of chromosome 7 or monosomy 7. Patients with EVI1^{High} AML exhibit specific clinical features, including elevated platelet counts, association with monosomy 7 or chromosome 7 deletion, refractoriness to therapy and a poor prognosis.[43] It has been suggested that the genomic instability and myelodysplasia with monosomy 7 occur as a consequence of EVI1 activation after gene therapy for chronic granulomatous disease.[44] It seems likely that EVI1 and gene(s) on chromosome 7 play a crucial role in regulating CD52 expression. We have previously shown that EVI1 is expressed on bone marrow stem and progenitor cells and has an important function in maintaining hematopoietic stem cells.[45] It is, therefore, tempting to speculate that specific stem cell populations may express CD52 along with EVI1. Future studies should examine the expression of CD52 on hematopoietic stem cells and its relevance to leukemia development. It is also important to determine whether EVI1 directly activates the CD52 promoter.

Although the mechanism of cytotoxicity of CAMPATH-1H is not well understood, CAMPATH-1H had minimal direct cytotoxicity, but exhibited significant CDC against chronic lymphocytic leukemia and acute lymphocytic leukemia cells.[18,19] In our experiments, CAMPATH-1H lysed EVI1^{High} AML cells more efficiently through direct cytotoxicity or ADCC than through CDC (Figures 3 and 4). CD52 is a 12-amino-acid glycopolypeptide containing a large glucose moiety, and CAMPATH-1H recognizes C-terminal amino acids and part of the glycosylphosphatidylinositol anchor of CD52.[46,47] The amount of protein and/or post-translational modifications, such as glycosylation, may be involved in differential immune responses to CAMPATH-1H.

We showed that EVI1^{High} AML cells are good targets for the cytolytic activity of CAMPATH-1H. In the standard schedule of CAMPATH-1H for allogeneic stem cell transplantation, the treatment is not always efficient because the antibody adsorbs onto T lymphocytes. Therefore, combinations of CAMPATH-1H with active chemotherapeutic agents such as daunorubicin, etoposide and cytarabine need to be explored in future studies. Finally, these studies provide support for a clinical trial of CAMPATH-1H in patients with EVI1^{High} AML and potentially in patients with other AMLs that express CD52.

Conflict of interest

The authors declare no conflict of interest.

Acknowledgements

We gratefully acknowledge Genzyme for providing the CAMPATH-1H antibody for the study.

References

1 Morishita K, Parker DS, Mucenski ML, Jenkins NA, Copeland NG, Ihle JN. Retroviral activation of a novel gene encoding a zinc finger protein in IL-3-dependent myeloid leukemia cell lines. *Cell* 1988; **54**: 831–840.
2 Mucenski ML, Taylor BA, Ihle JN, Hartley JW, Morse III HC, Jenkins NA *et al*. Identification of a common ecotropic viral integration site, Evi-1, in the DNA of AKXD murine myeloid tumors. *Mol Cell Biol* 1988; **8**: 301–308.
3 Morishita K, Parganas E, William CL, Whittaker MH, Drabkin H, Oval J *et al*. Activation of EVI1 gene expression in human acute myelogenous leukemias by translocations spanning 300–400

kilobases on chromosome band 3q26. *Proc Natl Acad Sci USA* 1992; **89**: 3937–3941.
4 Mitani K, Ogawa S, Tanaka T, Miyoshi H, Kurokawa M, Mano H *et al.* Generation of the AML1-EVI-1 fusion gene in the t(3;21)(q26;q22) causes blastic crisis in chronic myelocytic leukemia. *EMBO J* 1994; **13**: 504–510.
5 Lugthart S, Groschel S, Beverloo HB, Kayser S, Valk PJ, van Zelderen-Bhola SL *et al.* Clinical, molecular, and prognostic significance of WHO type inv(3)(q21q26.2)/t(3;3)(q21;q26.2) and various other 3q abnormalities in acute myeloid leukemia. *J Clin Oncol* 2010; **28**: 3890–3898.
6 Barjesteh van Waalwijk van Doorn-Khosrovani S, Erpelinck C, van Putten WL, Valk PJ, van der Poel-van de Luytgaarde S, Hack R *et al.* High EVI1 expression predicts poor survival in acute myeloid leukemia: a study of 319 *de novo* AML patients. *Blood* 2003; **101**: 837–845.
7 Lugthart S, van Drunen E, van Norden Y, van Hoven A, Erpelinck CA, Valk PJ *et al.* High EVI1 levels predict adverse outcome in acute myeloid leukemia: prevalence of EVI1 overexpression and chromosome 3q26 abnormalities underestimated. *Blood* 2008; **111**: 4329–4337.
8 Groschel S, Lugthart S, Schlenk RF, Valk PJ, Eiwen K, Goudswaard C *et al.* High EVI1 expression predicts outcome in younger adult patients with acute myeloid leukemia and is associated with distinct cytogenetic abnormalities. *J Clin Oncol* 2010; **28**: 2101–2107.
9 Xia MQ, Tone M, Packman L, Hale G, Waldmann H. Characterization of the CAMPATH-1 (CDw52) antigen: biochemical analysis and cDNA cloning reveal an unusually small peptide backbone. *Eur J Immunol* 1991; **21**: 1677–1684.
10 Valentin H, Gelin C, Coulombel L, Zoccola D, Morizet J, Bernard A. The distribution of the CDW52 molecule on blood cells and characterization of its involvement in T cell activation. *Transplantation* 1992; **54**: 97–104.
11 Xia MQ, Hale G, Lifely MR, Ferguson MA, Campbell D, Packman L *et al.* Structure of the CAMPATH-1 antigen, a glycosylphosphatidylinositol-anchored glycoprotein which is an exceptionally good target for complement lysis. *Biochem J* 1993; **293**: 633–640.
12 Osterborg A, Dyer MJ, Bunjes D, Pangalis GA, Bastion Y, Catovsky D *et al.* Phase II multicenter study of human CD52 antibody in previously treated chronic lymphocytic leukemia. European Study Group of CAMPATH-1H Treatment in Chronic Lymphocytic Leukemia. *J Clin Oncol* 1997; **15**: 1567–1574.
13 Rodig SJ, Abramson JS, Pinkus GS, Treon SP, Dorfman DM, Dong HY *et al.* Heterogeneous CD52 expression among hematologic neoplasms: implications for the use of alemtuzumab (CAMPATH-1H). *Clin Cancer Res* 2006; **12**: 7174–7179.
14 Tibes R, Keating MJ, Ferrajoli A, Wierda W, Ravandi F, Garcia-Manero G *et al.* Activity of alemtuzumab in patients with CD52-positive acute leukemia. *Cancer* 2006; **106**: 2645–2651.
15 Alinari L, Lapalombella R, Andritsos L, Baiocchi RA, Lin TS, Byrd JC. Alemtuzumab (Campath-1H) in the treatment of chronic lymphocytic leukemia. *Oncogene* 2007; **26**: 3644–3653.
16 Hale C, Bartholomew M, Taylor V, Stables J, Topley P, Tite J. Recognition of CD52 allelic gene products by CAMPATH-1H antibodies. *Immunology* 1996; **88**: 183–190.
17 Hale G. The CD52 antigen and development of the CAMPATH antibodies. *Cytotherapy* 2001; **3**: 137–143.
18 Zent CS, Chen JB, Kurten RC, Kaushal GP, Lacy HM, Schichman SA. Alemtuzumab (CAMPATH 1H) does not kill chronic lymphocytic leukemia cells in serum free medium. *Leuk Res* 2004; **28**: 495–507.
19 Golay J, Cortiana C, Manganini M, Cazzaniga G, Salvi A, Spinelli O *et al.* The sensitivity of acute lymphoblastic leukemia cells carrying the t(12;21) translocation to campath-1H-mediated cell lysis. *Haematologica* 2006; **91**: 322–330.
20 Greenwood J, Clark M, Waldmann H. Structural motifs involved in human IgG antibody effector functions. *Eur J Immunol* 1993; **23**: 1098–1104.
21 Zhang Z, Zhang M, Goldman CK, Ravetch JV, Waldmann TA. Effective therapy for a murine model of adult T-cell leukemia with the humanized anti-CD52 monoclonal antibody, Campath-1H. *Cancer Res* 2003; **63**: 6453–6457.
22 Golay J, Manganini M, Rambaldi A, Introna M. Effect of alemtuzumab on neoplastic B cells. *Haematologica* 2004; **89**: 1476–1483.
23 Stanglmaier M, Reis S, Hallek M. Rituximab and alemtuzumab induce a nonclassic, caspase-independent apoptotic pathway in B-lymphoid cell lines and in chronic lymphocytic leukemia cells. *Ann Hematol* 2004; **83**: 634–645.
24 Mone AP, Cheney C, Banks AL, Tridandapani S, Mehter N, Guster S *et al.* Alemtuzumab induces caspase-independent cell death in human chronic lymphocytic leukemia cells through a lipid raft-dependent mechanism. *Leukemia* 2006; **20**: 272–279.
25 Oval J, Smedsrud M, Taetle R. Expression and regulation of the evi-1 gene in the human factor-dependent leukemia cell line, UCSD/AML1. *Leukemia* 1992; **6**: 446–451.
26 Oval J, Jones OW, Montoya M, Taetle R. Characterization of a factor-dependent acute leukemia cell line with translocation (3;3)(q21;q26). *Blood* 1990; **76**: 1369–1374.
27 Strefford JC, Foot NJ, Chaplin T, Neat MJ, Oliver RT, Young BD *et al.* The characterisation of the lymphoma cell line U937, using comparative genomic hybridisation and multiplex FISH. *Cytogenet Cell Genet* 2001; **94**: 9–14.
28 Gribble SM, Roberts I, Grace C, Andrews KM, Green AR, Nacheva EP. Cytogenetics of the chronic myeloid leukemia-derived cell line K562: karyotype clarification by multicolor fluorescence *in situ* hybridization, comparative genomic hybridization, and locus-specific fluorescence *in situ* hybridization. *Cancer Genet Cytogenet* 2000; **118**: 1–8.
29 Koeffler HP, Billing R, Lusis AJ, Sparkes R, Golde DW. An undifferentiated variant derived from the human acute myelogenous leukemia cell line (KG-1). *Blood* 1980; **56**: 265–273.
30 MacLeod RA, Dirks WG, Drexler HG. Early contamination of the Dami cell line by HEL. *Blood* 1997; **90**: 2850–2851.
31 Gallagher R, Collins S, Trujillo J, McCredie K, Ahearn M, Tsai S *et al.* Characterization of the continuous, differentiating myeloid cell line (HL-60) from a patient with acute promyelocytic leukemia. *Blood* 1979; **54**: 713–733.
32 Tsuchiya S, Yamabe M, Yamaguchi Y, Kobayashi Y, Konno T, Tada K. Establishment and characterization of a human acute monocytic leukemia cell line (THP-1). *Int J Cancer* 1980; **26**: 171–176.
33 Hamaguchi H, Suzukawa K, Nagata K, Yamamoto K, Yagasaki F, Morishita K. Establishment of a novel human myeloid leukaemia cell line (HNT-34) with t(3;3)(q21;q26), t(9;22)(q34;q11) and the expression of EVI1 gene, P210 and P190 BCR/ABL chimaeric transcripts from a patient with AML after MDS with 3q21q26 syndrome. *Br J Haematol* 1997; **98**: 399–407.
34 Matsuo Y, Adachi T, Tsubota T, Imanishi J, Minowada J. Establishment and characterization of a novel megakaryoblastic cell line, MOLM-1, from a patient with chronic myelogenous leukemia. *Hum Cell* 1991; **4**: 261–264.
35 Asou H, Suzukawa K, Kita K, Nakase K, Ueda H, Morishita K *et al.* Establishment of an undifferentiated leukemia cell line (Kasumi-3) with t(3;7)(q27;q22) and activation of the EVI1 gene. *Jpn J Cancer Res* 1996; **87**: 269–274.
36 Suzukawa K, Kodera T, Shimizu S, Nagasawa T, Asou H, Kamada N *et al.* Activation of EVI1 transcripts with chromosomal translocation joining the TCRVbeta locus and the EVI1 gene in human acute undifferentiated leukemia cell line (Kasumi-3) with a complex translocation of der(3)t(3;7;8). *Leukemia* 1999; **13**: 1359–1366.
37 Abo J, Inokuchi K, Dan K, Nomura T. p53 and N-ras mutations in two new leukemia cell lines established from a patient with multilineage CD7-positive acute leukemia. *Blood* 1993; **82**: 2829–2836.
38 Hamaguchi H, Nagata K, Yamamoto K, Fujikawa I, Kobayashi M, Eguchi M. Establishment of a novel human myeloid leukaemia cell line (FKH-1) with t(6;9)(p23;q34) and the expression of dek-can chimaeric transcript. *Br J Haematol* 1998; **102**: 1249–1256.
39 Hamaguchi H, Inokuchi K, Nara N, Nagata K, Yamamoto K, Yagasaki F *et al.* Alterations in the colorectal carcinoma gene and protein in a novel human myeloid leukemia cell line with trisomy 18 established from overt leukemia after myelodysplastic syndrome. *Int J Hematol* 1998; **67**: 153–164.
40 Pawson R, Dyer MJ, Barge R, Matutes E, Thornton PD, Emmett E *et al.* Treatment of T-cell prolymphocytic leukemia with human CD52 antibody. *J Clin Oncol* 1997; **15**: 2667–2672.
41 Piccaluga PP, Agostinelli C, Righi S, Zinzani PL, Pileri SA. Expression of CD52 in peripheral T-cell lymphoma. *Haematologica* 2007; **92**: 566–567.

42 Geissinger E, Bonzheim I, Roth S, Rosenwald A, Muller-Hermelink HK, Rudiger T. CD52 expression in peripheral T-cell lymphomas determined by combined immunophenotyping using tumor cell specific T-cell receptor antibodies. *Leuk Lymphoma* 2009; **50**: 1010–1016.
43 Lugthart S, Gröschel S, Beverloo HB, Kayser S, Valk PJ, van Zelderen-Bhola SL *et al.* Clinical, molecular, and prognostic significance of WHO type inv(3)(q21q26.2)/t(3;3)(q21;q26.2) and various other 3q abnormalities in acute myeloid leukemia. *J Clin Oncol* 2010; **28**: 3890–3898.
44 Stein S, Ott MG, Schultze-Strasser S, Jauch A, Burwinkel B, Kinner A *et al.* Genomic instability and myelodysplasia with monosomy 7 consequent to EVI1 activation after gene therapy for chronic granulomatous disease. *Nat Med* 2010; **16**: 198–204.
45 Yuasa H, Oike Y, Iwama A, Nishikata I, Sugiyama D, Perkins A *et al.* Oncogenic transcription factor Evi1 regulates hematopoietic stem cell proliferation through GATA-2 expression. *EMBO J* 2005; **24**: 1976–1987.
46 Treumann A, Lifely MR, Schneider P, Ferguson MA. Primary structure of CD52. *J Biol Chem* 1995; **270**: 6088–6099.
47 Ermini L, Secciani F, La Sala GB, Sabatini L, Fineschi D, Hale G *et al.* Different glycoforms of the human GPI-anchored antigen CD52 associate differently with lipid microdomains in leukocytes and sperm membranes. *Biochem Biophys Res Commun* 2005; **338**: 1275–1283.

Supplementary Information accompanies the paper on the Leukemia website (http://www.nature.com/leu)

J Nat Med (2011) 65:651–655
DOI 10.1007/s11418-011-0510-5

NATURAL RESOURCE LETTER

Inhibition of proliferation by agricultural plant extracts in seven human adult T-cell leukaemia (ATL)-related cell lines

Hisahiro Kai · Ena Akamatsu · Eri Torii · Hiroko Kodama · Chizuko Yukizaki · Yoichi Sakakibara · Masahito Suiko · Kazuhiro Morishita · Hiroaki Kataoka · Koji Matsuno

Received: 4 November 2010 / Accepted: 30 December 2010 / Published online: 4 February 2011

Abstract Adult T-cell leukaemia (ATL) is caused by human T-cell leukaemia virus type I (HTLV-I) infection and is resistant to conventional chemotherapy. We evaluated the inhibitory effects of agricultural plants on the proliferation of seven ATL-related human leukaemia cells, using three ATL cell lines (ED, Su9T01 and S1T), two human T-cell lines transformed by HTLV-I infection (HUT-102 and MT-2) and two HTLV-I-negative human T-cell acute lymphoblastic leukaemia cell lines (Jurkat and MOLT-4). A total of 52 samples of 80% ethanol extracts obtained from 30 types of agricultural plants were examined. On the basis of IC_{50} values, we selected samples with greater activity than genistein, which was used as a positive control. The highest inhibitory effect was observed with extracts from leaves of *Vaccinium virgatum* Aiton (blueberry) on four cell lines (ED, Su9T01, HUT-102 and Jurkat); seeds of *Momordica charantia* L. (bitter gourd) exhibited the second highest activity. The bitter gourd seeds suppressed the proliferation of three cell lines (Su9T01, HUT-102 and Jurkat). The extracts from edible parts of *Ipomea batatas* LAM. (sweet potato), edible parts of *Colocasia esculenta* (L.) Schott (taro), skin of taro and seeds of *Prunus mume* Sieb. et Zucc. (mume) showed markedly greater inhibitory effects on Su9T01 than genistein. These findings suggest that ATL-preventative bioactive compounds may exist in these agricultural plants, which are considered to be functional foods.

Keywords Screening · Agricultural plants · Adult T-cell leukaemia (ATL) · Human T-lymphotropic virus type I (HTLV-I)

Introduction

Adult T-cell leukaemia (ATL) occurs in a small population of individuals infected with human T-cell leukaemia virus type I (HTLV-I). After infection with HTLV-I, 2–5% of

H. Kai · K. Matsuno (✉)
Department of Pharmaceutical Health Sciences,
School of Pharmaceutical Sciences, Kyushu University of Health and Welfare, 1714-1 Yoshino-machi,
Nobeoka, Miyazaki 882-8508, Japan
e-mail: kjmtsn@phoenix.ac.jp

H. Kai · E. Akamatsu · E. Torii · H. Kodama
Research Promotion Bureau for Collaboration of Regional Entities, Miyazaki Prefectural Industrial Support Foundation,
16500-2 Higashi-Kaminaka, Sadowara-cho,
Miyazaki 880-0303, Japan

C. Yukizaki
Miyazaki Prefectural Food Research and Development Center,
16500-2 Higashi-Kaminaka, Sadowara-cho,
Miyazaki 880-0303, Japan

Y. Sakakibara · M. Suiko
Department of Biochemistry and Applied Biosciences,
Faculty of Agriculture, University of Miyazaki,
1-1 Gakuenkibanadai-nishi, Miyazaki 889-2192, Japan

K. Morishita
Division of Tumor and Cellular Biochemistry,
Department of Medical Sciences, Faculty of Medicine,
University of Miyazaki, 5200 Kihara Kiyotake,
Miyazaki 889-1692, Japan

H. Kataoka
Section of Oncopathology and Regenerative Biology,
Department of Pathology, Faculty of Medicine,
University of Miyazaki, 5200 Kihara Kiyotake,
Miyazaki 889-1692, Japan

carriers are likely to develop ATL after a long latency period (30–50 years) [1]. The affected patients are frequently from certain areas of Japan, South America, the Caribbean Basin, West Central Africa, northern Iran, southern India and other isolated tropical regions [2]. In Japan, the prevalence rate has reached 37% of the population in the southern and western parts of Kyushu (i.e. Miyazaki, Kagoshima and Nagasaki Prefectures) [3]. ATL has a poor prognosis, with a mean survival time of 13 months, being refractory to currently available combination chemotherapy [4]. Therefore, it is important to continue the search for an appropriate therapeutic method to prevent the development of ATL or to prolong survival after its occurrence. Recent studies reported that certain components of natural foods, such as curcumin [5], capsaicin [6], soy-derived isoflavones [7], epigallocatechin-3-gallate [8], a derivative compound of imidazoquinoxaline [9] and brown algae fucoxanthin [10], have inhibitory effects on ATL cell line growth. However, there are no reports of large screening tests of ATL cell line growth using a multitude of agricultural plants; such tests may potentially reveal the existence of several kinds of active compounds. In the present study, we screened 52 samples of agricultural plants for their ability to inhibit proliferation in seven leukaemia cell lines (three ATL cell lines, two human T-cell lines transformed by HTLV-I infection and two HTLV-I-negative human T-cell acute lymphoblastic leukaemia cell lines) to identify useful drugs for the prevention and/or treatment of ATL.

Materials and methods

Agricultural plant extracts

All agricultural plants were cultivated at the Miyazaki Agricultural Research Institute. The scientific names of all samples were identified by Dr H. Kunitake (Miyazaki University, Japan). The fresh agricultural plants were separated into their parts (i.e. bulb, core, edible parts, flesh, flower, fruits, hull, leaves, peel, pericarp, placenta, roots, seeds, skin and stems), freeze-dried and powdered. The freeze-dried powders (1 g) were extracted with 30 ml of 80% ethanol. The extracts were evaporated, dissolved in methanol or dimethyl sulfoxide and subjected to assay screening. Samples of the agricultural plants used in these experiments were stored at the Miyazaki Prefectural Food Research and Development Center (MFDC). Voucher specimens were also deposited at MFDC. Collection dates are shown in Table 1.

Cell culture

ED cells were kindly provided by Dr M. Maeda (Kyoto University, Japan) and Su9T01 and S1T cells were kindly provided by Dr N. Arima (Kagoshima University, Japan) [11]. HUT-102, MT-2, Jurkat and MOLT-4 cells were obtained from the Fujisaki Cell Center, Hayashibara Biochemical Laboratories (Okayama, Japan). All cells were maintained in RPMI 1640 medium (Sigma, St. Louis, MO, USA) supplemented with 10% fetal bovine serum (SAFC Biosciences, Lenexa, KS, USA, lot no. 3M0469) containing 100 U/ml penicillin G and 100 μg/ml streptomycin (Sigma, St. Louis, MO, USA). Each cell line was subcultured twice a week, and in the actual in vitro experiment, the cell number was adjusted to 1×10^5 cells/ml.

Cell proliferation assay

Each cell line was seeded (1×10^5 cells/ml, 90 μl/well) into a 96-well plate containing RPMI 1640 medium. After incubation at 37°C for 24 h in an atmosphere of 5% CO_2, the samples were added (10 μl/well) and subsequently incubated for an additional 72 h. The inhibition of cell proliferation was determined using a 2-(2-methoxy-4-nitrophenyl)-3-(4-nitrophenyl)-5-(2,4-disulfophenyl)-2*H*-tetrazolium monosodium salt (WST-8) assay kit (Dojindo, Kumamoto, Japan). Each cell line was incubated with individual extracts for 72 h and the viable cells were detected using a WST-8 assay kit. The viable cells convert the tetrazolium salt in WST-8 to a highly water soluble formazan. The concentration at which cell proliferation is inhibited by 50% compared to an untreated control is expressed as IC_{50}. Genistein (Wako, Osaka, Japan) was used as a positive control [7].

Results

Table 1 shows the agricultural plants, parts and voucher numbers of the 52 samples. All samples extracted with 80% ethanol were screened for proliferation inhibitory activity in ATL cell lines (ATL group: ED, Su9T01 and S1T), human T-cell lines transformed by HTLV-I infection (HTLV-I group: MT-2 and HUT-102) and HTLV-I-negative human T-cell acute lymphoblastic leukaemia cell lines (non-HTLV-I group: Jurkat and MOLT-4). Table 2 shows the samples with the greatest inhibitory activity based on IC_{50} values (μg/ml); genistein was used as a positive control [7].

In the ATL group, only blueberry leaves (no. 8: $IC_{50} = 10.5$ μg/ml) had a greater inhibitory effect than genistein ($IC_{50} = 19.8$ μg/ml) on ED cells. In Su9T01 cells, bitter gourd seeds, blueberry leaves, edible parts of sweet potato, edible parts of taro, taro skin and mume seeds (nos. 4, 8, 42, 47, 48 and 51: $IC_{50} = 0.3$, 5.4, 6.0, 26.2, 45.0 and 45.9 μg/ml, respectively) had greater inhibitory effects than genistein ($IC_{50} = 58.1$ μg/ml). However, no samples exhibited greater inhibitory activity than genistein ($IC_{50} = 11.3$ μg/ml) on S1T cells.

Table 1 List of agricultural plants, parts, voucher numbers and collection dates

No.	Scientific name	Common name	Parts	Voucher number	Collection date
1	*Capsicum annuum* L.	Bell pepper (green colour)	Edible parts	Mi-CREATE-01	March 2003
2			Placenta	Mi-CREATE-02	March 2003
3	*Capsicum annuum* L.	Bell pepper (orange colour)	Fruits	Mi-CREATE-03	April 2003
4	*Momordica charantia* L.	Bitter gourd	Seeds	Mi-CREATE-04	August 2003
5			Pericarp	Mi-CREATE-05	August 2003
6			Placenta	Mi-CREATE-06	August 2003
7	*Oryza sativa* L.	Black rice	Edible parts	Mi-CREATE-07	September 2003
8	*Vaccinium virgatum* Aiton	Blueberry	Leaves	Mi-CREATE-08	August 2004
9	*Arctium lappa* L.	Edible burdock	Root with skin	Mi-CREATE-09	October 2004
10	*Daucas carota* L.	Carrot	Root with skin	Mi-CREATE-10	January 2004
11			Leaves	Mi-CREATE-11	January 2004
12	*Chamaemelum nobile* (L.) All.	Chamomile	Flower	Mi-CREATE-12	May 2003
13	*Capsicum chinense* L.	Chilli pepper	Pericarp	Mi-CREATE-13	April 2004
14			Placenta, seeds	Mi-CREATE-14	April 2004
15	*Citrus* spp.	Citrus (Soyomizu)	Seeds	Mi-CREATE-15	May 2003
16			Peel	Mi-CREATE-16	May 2003
17			Segments, albedo	Mi-CREATE-17	May 2003
18	*Solanum melongena* L.	Eggplant	Fruits	Mi-CREATE-18	August 2003
19	*Petroselinum crispum* (Mill.) var. neapolitanum	Italian parsley	Leaves	Mi-CREATE-19	July 2003
20	*Raphanus sativus* (L.) var. longipinnatus	Japanese radish	Root with skin	Mi-CREATE-20	January 2004
21			Leaves	Mi-CREATE-21	January 2004
22	*Fortunella crassifolia* Swingle	Kumquat	Edible parts (ripe)	Mi-CREATE-22	March 2004
23			Seeds (ripe)	Mi-CREATE-23	March 2004
24			Edible parts (immature)	Mi-CREATE-24	October 2003
25			Seeds (immature)	Mi-CREATE-25	October 2003
26	*Lactuca sativa* L. Capitata Group	Head lettuce	Edible parts	Mi-CREATE-26	March 2004
27	*Mangifera indica* L.	Mango	Flesh	Mi-CREATE-27	July 2003
28			Skin	Mi-CREATE-28	July 2003
29	*Cucumis melo* L. var. reticulatus Naud.	Netted melon	Fruits	Mi-CREATE-29	December 2003
30			Placenta, seeds	Mi-CREATE-30	December 2003
31	*Allium cepa* L.	Onion	Bulb	Mi-CREATE-31	March 2004
32			Leaves	Mi-CREATE-32	March 2004
33	*Elatostema involucratum* Franch. & Sar.	Potherb mustard	Leaves	Mi-CREATE-33	April 2004
34	*Glycine max* Merrill	Soybean	Whole beans	Mi-CREATE-34	May 2004
35	*Pisum sativum* L.	Pea	Hull	Mi-CREATE-35	April 2004
36			Leaves, stem	Mi-CREATE-36	April 2004
37			Whole beans	Mi-CREATE-37	April 2004
38	*Cucurbita* spp.	Cushaw	Edible parts	Mi-CREATE-38	February 2004
39			Seeds, placenta	Mi-CREATE-39	February 2004
40	*Stevia rebaudiana* Bertoni	Stevia	Leaves	Mi-CREATE-40	July 2003
41	*Fragaria x ananassa* Duchesne	Strawberry	Fruits	Mi-CREATE-41	April 2003
42	*Ipomea batatas* LAM.	Sweet potato	Edible parts	Mi-CREATE-42	October 2003
43			Stems	Mi-CREATE-43	October 2003
44			Leaves	Mi-CREATE-44	October 2003
45	*Zea mays* L.	Sweet corn	Immature kernels	Mi-CREATE-45	May 2003

Table 1 continued

No.	Scientific name	Common name	Parts	Voucher number	Collection date
46			Core	Mi-CREATE-46	May 2003
47	*Colocasia esculenta* (L.) Schott	Taro	Edible parts	Mi-CREATE-47	October 2003
48			Skin	Mi-CREATE-48	October 2003
49	*Lycopersicum esculentum* Mill. var. cerasiforme	Tomato	Fruits	Mi-CREATE-49	April 2003
50	*Prunus mume Sieb.* et Zucc.	Mume	Flesh	Mi-CREATE-50	May 2003
51			Seeds	Mi-CREATE-51	May 2003
52	*Cucurbita pepo* L.	Zucchini	Fruits	Mi-CREATE-52	February 2003

In the HTLV-I group, bitter gourd seeds and blueberry leaves (nos. 4 and 8: $IC_{50} = 24.0$ and 17.3 μg/ml, respectively) had greater inhibitory effects than genistein ($IC_{50} = 28.2$ μg/ml) on HUT-102 cells. However, there were no samples with greater activity than genistein ($IC_{50} = 14.1$ μg/ml) on MT-2 cells.

In the non-HTLV-I group, bitter gourd and blueberry leaves (nos. 4 and 8: $IC_{50} = 32.7$ and 15.7 μg/ml, respectively) had greater inhibitory effects than genistein ($IC_{50} = 33.1$ μg/ml) on Jurkat cells. However, there were no samples with greater inhibitory activity than genistein ($IC_{50} \doteq 31.5$ μg/ml) on MOLT-4 cells.

Overall, these results show that bitter gourd seeds (no. 4) and blueberry leaves (no. 8) had significant inhibitory effects in these seven leukaemia cell lines. Other samples showed weak inhibition in these seven leukaemia cell lines, with most of the IC_{50} values being greater than 100 μg/ml (data not shown).

Discussion

We examined the inhibitory effects of 52 agricultural plant extracts on the proliferation of seven ATL-related cell lines. The results were compared with the inhibitory effect of genistein (positive control). Genistein is a soy-derived isoflavone and is known to have several bioactivities [12]; we confirmed that genistein inhibits the proliferation of seven ATL-related cell lines. In particular, the extracts from blueberry leaves and bitter gourd seeds exhibited greater inhibitory potencies than the control towards Su9T01, HUT-102 and Jurkat cells. In addition, blueberry leaves also exhibited potent inhibitory effects on ED cell proliferation (Table 2).

Matsuo et al. [13] reported that the polyphenols of rabbiteye blueberry leaves were mainly composed of proanthocyanidins, followed by caffeoylquinic acids and flavonol glycosides. Li et al. [8] reported that epigallocatechin-3-gallate inhibits proliferation of ATL, as well as HTLV-I infected cells, by suppressing HTLV-I pX gene expression and inducing apoptotic cell death. From these reports, proanthocyanidins may have contributed to the inhibitory effect on cell proliferation in ATL and HTLV-I infected cells.

Kobari et al. [14] reported that (9*Z*,11*E*,13*E*)-9,11,13-octadecatrienoic acid (α-eleostearic acid), which is one of the major fatty acids in bitter gourd seeds, as well as its dihydroxy derivative, inhibited the proliferation of HL60

Table 2 Inhibitory activity of 80% EtOH extracts from agricultural plants on cell proliferation in ATL-related leukaemia cell lines

No.	Scientific name	Common name	Parts	IC_{50} value (μg/ml)						
				ATL			HTLV-1		non-HTLV-I	
				ED	Su9T01	S1T	HUT-102	MT-2	Jurkat	MOLT-4
4	*Momordica charantia* L.	Bitter gourd	Seeds	24.5	0.3	85.8	24.0	41.7	32.7	87.7
8	*Vaccinium virgatum* Aiton	Blueberry	Leaves	10.5	5.4	13.8	17.3	16.0	15.7	71.0
42	*Ipomea batatas* LAM.	Sweet potato	Edible parts	>500.0	6.0	>500.0	>500.0	>500.0	>500.0	295.2
47	*Colocasia esculenta* (L.) Schott	Taro	Edible parts	31.2	26.2	25.0	83.5	64.7	59.8	106.9
48	*Colocasia esculenta* (L.) Schott	Taro	Skin	62.2	45.0	66.6	189.9	141.2	200.4	>500.0
51	*Prunus mume Sieb.* et Zucc.	Mume	Seeds	42.2	45.9	114.1	263.6	320.1	252.0	>500.0
		Genistein (μg/ml)		19.8	58.1	11.3	28.2	14.1	33.1	31.5
		Genistein (μM)		73.3	215.3	42.0	104.3	52.4	122.6	116.7

leukaemia cells, HT29 colorectal carcinoma and other cancer and fibroblast cells. HL60 leukaemia cells, which are uninfected HTLV-I cells, have been used as a bioactive screening test to evaluate medicinal plants and functional food for a long time. In this screening test result, the bitter gourd seeds suppressed proliferation of Su9T01, HUT-102 and Jurkat cells. In these cells, it is possible that α-eleostearic acid may have contributed to the inhibitory effect on cell proliferation.

The extracts from edible parts of sweet potato, edible parts of taro, taro skin and mume seeds showed markedly greater inhibitory effects than genistein only in Su9T01 cells. These products could be useful in the search for new anti-leukaemia therapeutic agents, specific for Su9T01 cells. This result indicates that the constituents of these agricultural plants might affect a molecular mechanism unique to Su9T01 cells.

In this experiment, we found that several products showed potent inhibitory effects on ATL-leukaemia cell lines and we intend to identify the active compounds from these materials.

Acknowledgments This work was supported by a Grant-in-Aid from the Collaboration of Regional Entities for the Advancement of Technological Excellence (CREATE) from the Japanese Science and Technology Agency. We thank Prof. Michiyuki Maeda (Kyoto University) and Prof. Naomichi Arima (Kagoshima University) for supplying the cell lines. We thank Prof. Hisato Kunitake (Miyazaki University) for identifying the scientific names of all agricultural plants.

References

1. Arisawa K, Soda M, Endo S, Kurokawa K, Katamine S, Shimokawa I, Koba T, Takahashi T, Saito H, Doi H, Shirahama S (2000) Evaluation of adult T-cell leukemia/lymphoma incidence and its impact on non-Hodgkin lymphoma incidence in southwestern Japan. Int J Cancer 85:319–324
2. Proietti FA, Carneiro-Proietti AB, Catalan-Soares BC, Murphy EL (2005) Global epidemiology of HTLV-I infection and associated diseases. Oncogene 24:6058–6068
3. Mueller N, Okayama A, Stuver S, Tachibana N (1996) Findings from the Miyazaki Cohort Study. J Acquir Immune Defic Syndr Hum Retrovirol 13(Suppl 1):S2–S7
4. Yamada Y, Tomonaga M, Fukuda H, Hanada S, Utsunomiya A, Tara M, Sano M, Ikeda S, Takatsuki K, Kozuru M, Araki K, Kawano F, Niimi M, Tobinai K, Hotta T, Shimoyama M (2001) A new G-CSF-supported combination chemotherapy, LSG15, for adult T-cell leukaemia-lymphoma: Japan Clinical Oncology Group Study 9303. Br J Haematol 113:375–382
5. Tomita M, Kawakami H, Uchihara JN, Okudaira T, Masuda M, Takasu N, Matsuda T, Ohta T, Tanaka Y, Mori N (2006) Curcumin suppresses constitutive activation of AP-1 by downregulation of JunD protein in HTLV-1-infected T-cell lines. Leuk Res 30:313–321
6. Zhang J, Nagasaki M, Tanaka Y, Morikawa S (2003) Capsaicin inhibits growth of adult T-cell leukemia cells. Leuk Res 27:275–283
7. Yamasaki M, Fujita S, Ishiyama E, Mukai A, Madhyastha H, Sakakibara Y, Suiko M, Hatakeyama K, Nemoto T, Morishita K, Kataoka H, Tsubouchi H, Nishiyama K (2007) Soy-derived isoflavones inhibit the growth of adult T-cell leukemia cells in vitro and in vivo. Cancer Sci 98:1740–1746
8. Li HC, Yashiki S, Sonoda J, Lou H, Ghosh SK, Byrnes JJ, Lema C, Fujiyoshi T, Karasuyama M, Sonoda S (2000) Green tea polyphenols induce apoptosis in vitro in peripheral blood T lymphocytes of adult T-cell leukemia patients. Jpn J Cancer Res 91:34–40
9. Moarbess G, El-Hajj H, Kfoury Y, El-Sabban ME, Lepelletier Y, Hermine O, Deleuze-Masquéfa C, Bonnet PA, Bazarbachi A (2008) EAPB0203, a member of the imidazoquinoxaline family, inhibits growth and induces caspase-dependent apoptosis in T-cell lymphomas and HTLV-I-associated adult T-cell leukemia/lymphoma. Blood 111:3770–3777
10. Ishikawa C, Tafuku S, Kadekaru T, Sawada S, Tomita M, Okudaira T, Nakazato T, Toda T, Uchihara JN, Taira N, Ohshiro K, Yasumoto T, Ohta T, Mori N (2008) Anti-adult T-cell leukemia effects of brown algae fucoxanthin and its deacetylated product, fucoxanthinol. Int J Cancer 123:2702–2712
11. Sasaki H, Nishikata I, Shiraga T, Akamatsu E, Fukami T, Hidaka T, Kubuki Y, Okayama A, Hamada K, Okabe H, Murakami Y, Tsubouchi H, Morishita K (2005) Overexpression of a cell adhesion molecule, TSLC1, as a possible molecular marker for acute-type adult T-cell leukemia. Blood 105:1204–1213
12. Wegrzyn G, Jakobkiewicz BJ, Gabig CM, Piotrowska E, Narajczyk M, Kloska A, Malinowska M, Dziedzic D, Golebiewska I, Moskot M, Wegrzyn A (2010) Genistein: a natural isoflavone with a potential for treatment of genetic diseases. Biochem Soc Trans 38:695–701
13. Matsuo Y, Fujita Y, Ohnishi S, Tanaka T, Hirabaru H, Kai T, Sakaida H, Nishizono S, Kouno I (2010) Chemical constituents of the leaves of rabbiteye blueberry (*Vaccinium ashei*) and characterisation of polymeric proanthocyanidins containing phenylpropanoid units and A-type linkages. Food Chem 121:1073–1079
14. Kobari M, Ohnishi-Kameyama M, Akimoto Y, Yukizaki C, Yoshida M (2008) α-Eleostearic acid and its dihydroxy derivative are major apoptosis-inducing components of bitter gourd. J Agric Food Chem 56:10515–10520

UICC
global cancer control

IJC
International Journal of Cancer

Defective human T-lymphotropic virus Type 1 provirus in asymptomatic carriers

Hiroyuki Takenouchi[1], Kazumi Umeki[1], Daisuke Sasaki[2], Ikuo Yamamoto[1], Hajime Nomura[1], Ichiro Takajo[1], Shiro Ueno[1], Kunihiko Umekita[1], Shimeru Kamihira[2], Kazuhiro Morishita[3] and Akihiko Okayama[1]

[1] Department of Rheumatology, Infectious Diseases and Laboratory Medicine, University of Miyazaki, Miyazaki, Japan
[2] Department of Laboratory Medicine, Nagasaki University School of Medicine, Nagasaki, Japan
[3] Division of Tumor Biochemistry, Department of Biochemistry, University of Miyazaki, Miyazaki, Japan

Few studies have specifically examined defective provirus in asymptomatic human T-lymphotropic virus Type 1 (HTLV-1) carriers and its relation to proviral DNA loads (PVLs). To assess the significance of defective provirus in asymptomatic carriers, we examined PVLs in peripheral blood mononuclear cells of 208 asymptomatic HTLV-1 carriers. The mean PVLs determined using primers for the *pol* region were less than that for the *pX* region in these carriers. Analysis of seven carriers with high PVLs for the *pX* region but lower PVLs for the *pol* region showed that four had single nucleotide polymorphisms of proviral genomes for the *pol* region and three had HTLV-1-infected cells with defective provirus. Three carriers with defective provirus showed high PVLs at their initial screens, and PVLs increased after a 10- to 12-year interval in two carriers. Southern blot assay showed clonal expansion of HTLV-1-infected cells, and the predominant clones changed during the observation period. These data suggest that although HTLV-1-infected cells with defective provirus may have a growth advantage, the predominant clones of HTLV-1-infected cells do not always survive for many years in asymptomatic carriers.

Human T-lymphotropic virus Type 1 (HTLV-1) is the causative agent of adult T-cell leukemia/lymphoma (ATL) and a progressive neurological disease known as HTLV-1-associated myelopathy/tropical spastic paraparesis (HAM/TSP).[1–4] When an individual is infected by HTLV-1, the virus randomly integrates into the genome of affected T-cells in the form of a provirus.[5] The majority of HTLV-1 carriers are asymptomatic, and only a fraction of the number of carriers develops ATL after a long latent period.[6,7] It is thought that HTLV-1 infection drives the proliferation of T-cells, leading to the clonal expansion of HTLV-1-infected cells.[8–11] A high level of HTLV-1-infected cells is considered a risk factor for developing ATL.[12]

The complete HTLV-1 provirus is ~9 kb and contains the coding regions for core protein (*gag*), protease (*pro*), polymerase (*pol*), envelope protein (*env*), regulatory proteins, such as Tax and Rex, and some accessory molecules between 5′ and 3′ long-terminal repeats (LTRs).[5,13] It has been reported that defective provirus was detectable in approximately half of patients with ATL.[14–18] Tamiya *et al.* reported two types of genome deletion in defective provirus.[16] One form (*i.e.*, Type 1) retains both LTRs and lacks internal sequences, such as the *gag* and *pol* regions. The other form (*i.e.*, Type 2) has only the 3′ LTR, and the 5′ LTR and its flanking internal sequences are preferentially deleted. HTLV-1-infected cells harboring Type 2 defective virus were frequently found in patients with ATL.[18] Defective provirus has also been reported to be detectable in asymptomatic HTLV-1 carriers. Morozov *et al.* reported that defective provirus, which lacked large internal sequences, was detectable in 18 of 20 HTLV-1 carriers.[19] However, it has not yet been determined whether the HTLV-1-infected cells with defective provirus are maintained for a long time in asymptomatic carriers and whether the defective provirus is associated with the development of ATL.

In our study, to clarify the significance of defective provirus in asymptomatic carriers, the peripheral mononuclear cells (PBMCs) of 208 HTLV-1 carriers were screened for the presence of defective provirus. Long polymerase chain reaction (PCR) and Southern blot analysis were performed to determine the changes in clonality of HTLV-1-infected cells

Key words: HTLV-1, asymptomatic carrier, proviral DNA loads
Abbreviations: ATL: adult T-cell leukemia/lymphoma; CTL: cytotoxic T-lymphocytes; HBZ: HTLV-1 basic leucine zipper factor; HTLV-1: human T-lymphotropic virus Type 1; LTR: long-terminal repeat; PBMCs: peripheral mononuclear cells; PCR: polymerase chain reaction; PVLs: proviral DNA loads
Grant sponsors: Ministry of Education, Science, Sports and Culture, Japan, Miyazaki Prefecture Collaboration of Regional Entities for the Advancement of Technological Excellence, JST
DOI: 10.1002/ijc.25450
History: Received 29 Jan 2010; Accepted 28 Apr 2010; Online 12 May 2010
Correspondence to: Akihiko Okayama, Department of Rheumatology, Infectious Diseases and Laboratory Medicine, Faculty of Medicine, University of Miyazaki, 5200 Kihara, Kiyotake, Miyazaki 889-1692, Japan, Tel: +81-985-85-7284, Fax: +81-985-85-4709, E-mail: okayama@med.miyazaki-u.ac.jp

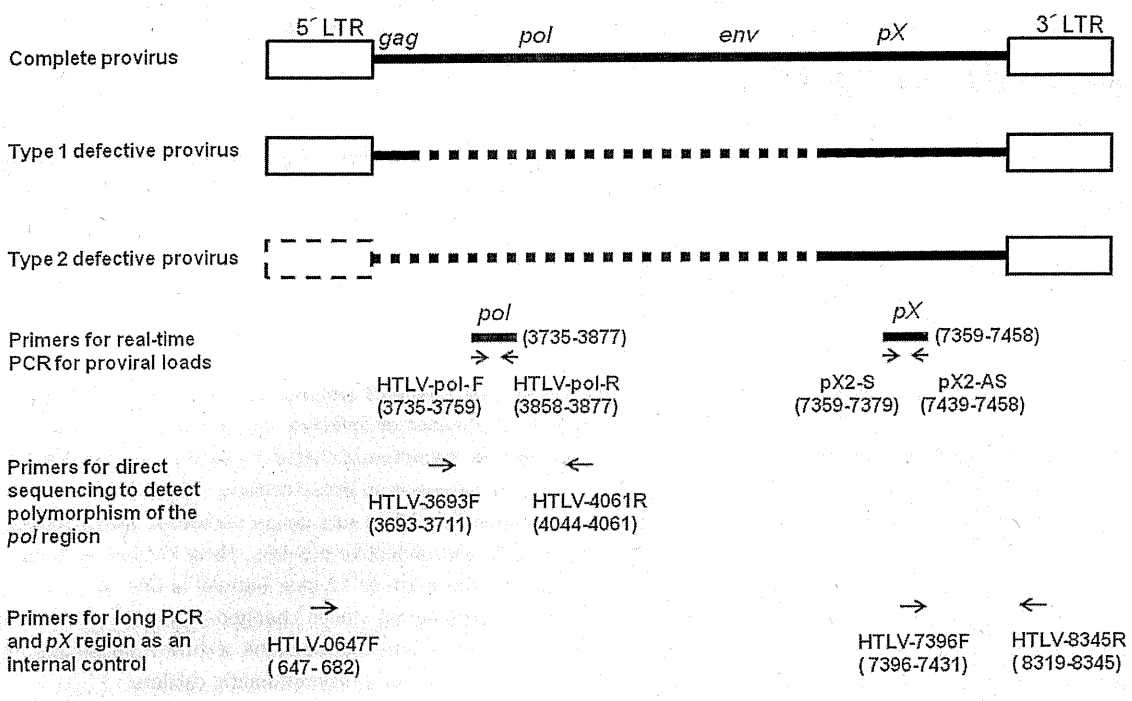

Figure 1. Schemas of structure of complete, Type 1 defective and Type 2 defective HTLV-1 (human T-lymphotropic virus Type 1) provirus. Dotted lines represent the defective regions of HTLV-1 provirus. Locations of primers for polymerase chain reactions in our study are revealed.

harboring defective provirus. Time-sequential samples of greater than 10 years obtained from asymptomatic carriers with large numbers of HTLV-1-positive cells with defective provirus were analyzed.

Material and Methods

Samples

Samples of PBMCs were obtained from 208 asymptomatic HTLV-1 carriers in the Miyazaki Cohort Study.[20] Informed consent was obtained from the study participants, and the study protocol was approved by the institutional review board at the University of Miyazaki. Genomic DNA was isolated from the PBMCs of HTLV-1 carriers by sodium dodecyl sulfate-proteinase K digestion, followed by phenol-chloroform extraction and ethanol precipitation.

Quantification of HTLV-1 provirus in PBMCs

Schemas of the structure of complete, Type 1 defective and Type 2 defective HTLV-1 provirus are shown in Figure 1.[16] The nucleotide position number of HTLV-1 provirus was according to Seiki *et al.* (accession no. J02029).[21]

Proviral DNA loads (PVLs) for the *pol* (positions 3735–3877) and *pX* (positions 7359–7458) regions were measured by real-time PCR using a Light Cycler DX 400 (Roche Diagnostics, Mannheim, Germany). When multiple time-sequential samples were available from one subject, the most recent sample was used for the first screening. The primers and the probe for the *pol* region of HTLV-1 provirus were as follows: the forward primer (HTLV-pol-F 5′-AACCAATT CATTCAAACATCTGACC-3′: positions 3735–3759), the reverse primer (HTLV-pol-R 5′-GCTTTCACAGGAGCCAA TGG-3′: positions 3877–3858) and the FAM-labeled probe (5′-FAM-TGTTCCTATCTTACTCCACCACAGTCACCGA-TA MRA-3′: positions 3767–3797).[22] The primers and the probe for the *pX* region of HTLV-1 provirus were as follows: the forward primer (pX2-S 5′-CGGATACCCAGTCTACGTGTT-3′: positions 7359–7379), the reverse primer (pX2-AS 5′-CAGTAGGG CGTGACGATGTA-3′: positions 7458–7439) and the FAM-labeled probe (5′-FAM-CTGTGTACAAGGCGACTGGTGCC-TAM RA-3′).[11] *RNase* P control Reagent (Applied Biosystems, Foster City, CA) was used for the primers and the probe for human *RNase* P DNA as internal control. PVLs were shown by the copy number of HTLV-1 provirus in 100 PBMCs.

Determination of DNA polymorphism in the *pol* primer region

To determine whether the lower PVLs for the *pol* region compared to that for the *pX* region in a same subject was due to the polymorphism of the DNA sequence of primers for the *pol* region, DNA sequence of PCR products of the *pol* region was identified in the cases described below. Primers used for PCR for this purpose were as follows: the forward primer (HTLV-3693F 5′-CTCTGCCAAACCATAC-3′: positions 3693–3711) and the reverse primer (HTLV-4061R 5′-ATGCAAAAGTCCGAGAAG-3′: positions 4061–4044). PCR products were supplied for direct sequencing using an

ABI PRISM Genetic Analyzer 310 (Applied Biosystems). To verify whether the polymorphism found affected the amplification efficiency of real-time PCR for measuring PVLs for the *pol* region, PCR products were subcloned by pGEM-T Easy vector system (Promega, Madison, WI). The amplification efficiency of real-time PCR for the *pol* region was compared between the DNA sequences with and without this polymorphism.

Detection of Type 1 defective provirus by long PCR

To assess whether the Type 1 defective provirus exists in the HTLV-1 carriers with lower PVLs for the *pol* region compared to those for the *pX* region, long PCR, which amplifies the complete provirus and the Type 1 defective provirus with 5′ LTR conserved, was performed. The primers were as follows: 5′LTR(HTLV-0647F 5′-GTTCCACCCCTTTCCCTTTC ATTCACGACTGACTGC-3′: positions 647–682) and 3′LTR (HTLV-8345R 5′-GGCTCTAAGCCCCCGGGGGATATTTG GGGCTCATGG-3′: positions 8345–8319).[18] Long PCR was performed using LA Taq DNA polymerase (Takara Bio, Shiga, Japan). Cycles for long PCR were as follows: one cycle of 98°C for 20 sec, 35 cycles of denaturation at 98°C for 10 sec, annealing at 65°C for 20 sec and extension at 72°C for 7 min. Genomic DNA containing 100 copies of HTLV-1 provirus for the *pX* region from each subject was used. To ensure that same amount of provirus was used for each reaction, PCR for the *pX* region was performed as an internal control. Primers used for this PCR were as follows: the forward primer (HTLV-7396F 5′-GGCGACTGGTGCCCCATCT CTGGGGGACTATGTTCG-3′: positions 7396–7431) and the reverse primer described above (HTLV-8345R).

DNA sequence analysis for Type 1 defective provirus

Long PCR products from subjects suspected of having defective provirus were subcloned by pGEM-T Easy vector system (Promega). The resulting plasmid DNA was purified by GenElute Plasmid Miniprep Kit (Sigma-Aldrich, St. Louis, MO). The DNA sequence of long PCR product was identified using an ABI PRISM Genetic Analyzer 310 (Applied Biosystems).

Southern blot hybridization analysis

To analyze the clonality of HTLV-1-infected cells, Southern blot analysis for HTLV-1 provirus was performed based on the method previously described by Kamihira *et al.* with slight modification.[17] Genomic DNA samples (10 μg) from cases were digested with restriction enzyme *Eco*RI (Fermentas, Barlington, Canada), electrophoresed on 0.7% agarose gel and transferred to nylon membrane (Roche). The filter was hybridized with DIG-PCR-labeled HTLV-1 DNA probe mix, which was prepared by a mixture of PCR products to cover the genome of 5′LTR-*gag* (positions 655–1624), *pro* (positions 2109–2619), *pol* (positions 3410–4059), *env* (positions 5464–6114) and *pX* (positions 7461–8646) and by incorporating DIG-11-dUTP (Roche). Finally, the band patterns were visualized with a CDP-star (Roche).

Results

PVLs of 208 asymptomatic HTLV-1 carriers based on the real-time PCR for the *pol* and *pX* regions

PVLs of 208 asymptomatic HTLV-1 carriers were determined by real-time PCR using primers for the *pol* and *pX* regions. The mean PVLs determined using primers for the *pol* region (2.3 copies per 100 PBMCs) were lower than that for the *pX* region (3.6 copies per 100 PBMCs). Because the *pX* region has been reported to be conserved in the HTLV-1 provirus,[14,16] the carriers, whose PVLs for the *pol* region were much lower than those for the *pX* region, were assumed to have many PBMCs harboring defective HTLV-1 provirus. Therefore, to characterize the carriers with defective HTLV-1 provirus, the subjects with relatively high PVLs for the *pX* region, which were equal to or greater than 1.0 copy per 100 PBMCs, and with PVLs for the *pol* region, which were less than half of those for the *pX* region, were supplied for further analysis. Seven carriers (Cases A–G) among 111 carriers with PVLs for the *pX* region, which were equal to or greater than 1.0 copy per 100 PBMCs, met this condition (Table 1).

DNA polymorphism analysis for the *pol* primer region

Although these seven carriers were potential carriers with relatively high PVLs and defective provirus, there was a possibility that the low PVLs for the *pol* region were due to the polymorphism of the DNA sequence of primers and probe for the *pol* region. Therefore, DNA sequences of the *pol* regions for PCR in Cases A–G were determined by the direct sequencing of PCR products. In Cases A–G, the polymorphism was not detected in the forward primer and probe annealing sequences. However, as shown in Table 1, the polymorphism of the DNA sequence was identified in two positions (3860 A>C and 3876 G>A) of the genome of provirus for the reverse primer for the *pol* region in four of seven cases (Cases D–G, Table 1). This DNA sequence was cloned into the plasmid, and the amplification efficacy of real-time PCR for the *pol* region was assessed. As expected, the amplification efficacy of real-time PCR in the plasmid with two nucleotide substitutions was ~3–4% of that in the plasmid without nucleotide substitutions (data not shown). These results accounted for the low PVLs for the *pol* region in Cases D–G shown in Table 1. Therefore, only Cases A–C were thought to potentially have many PBMCs with defective HTLV-1 provirus.

Sequential change of PVLs determined by real-time PCR for the *pol* and *pX* regions

All of three cases (Cases A, B and C) were followed-up for 10 or more years, and the samples from several screens were available (Fig. 2). None of these cases showed any signs or

Table 1. Proviral DNA loads for the *pol* and *pX* regions and polymorphism found in the *pol* region

Cases	Sex	Age (years)	PVLs (copies/100 PBMCs)			Polymorphism of *pol* region	
			pX	*pol*	*pX/pol*	3860[1]	3876[1]
A	Male	61	57.5	2.8	21.7	A	G
B	Female	73	31.7	0.5	59.2	A	G
C	Female	84	17.3	3.8	4.6	A	G
D	Male	82	12.6	0.4	5.5	C	A
E	Male	45	3.7	0.1	30.6	C	A
F	Male	75	2.5	0.1	27.2	C	A
G	Male	83	1.9	0.1	24.5	C	A

PVLs: proviral DNA loads; PBMCs: peripheral blood mononuclear cells.
[1]Position of proviral genome sequence.

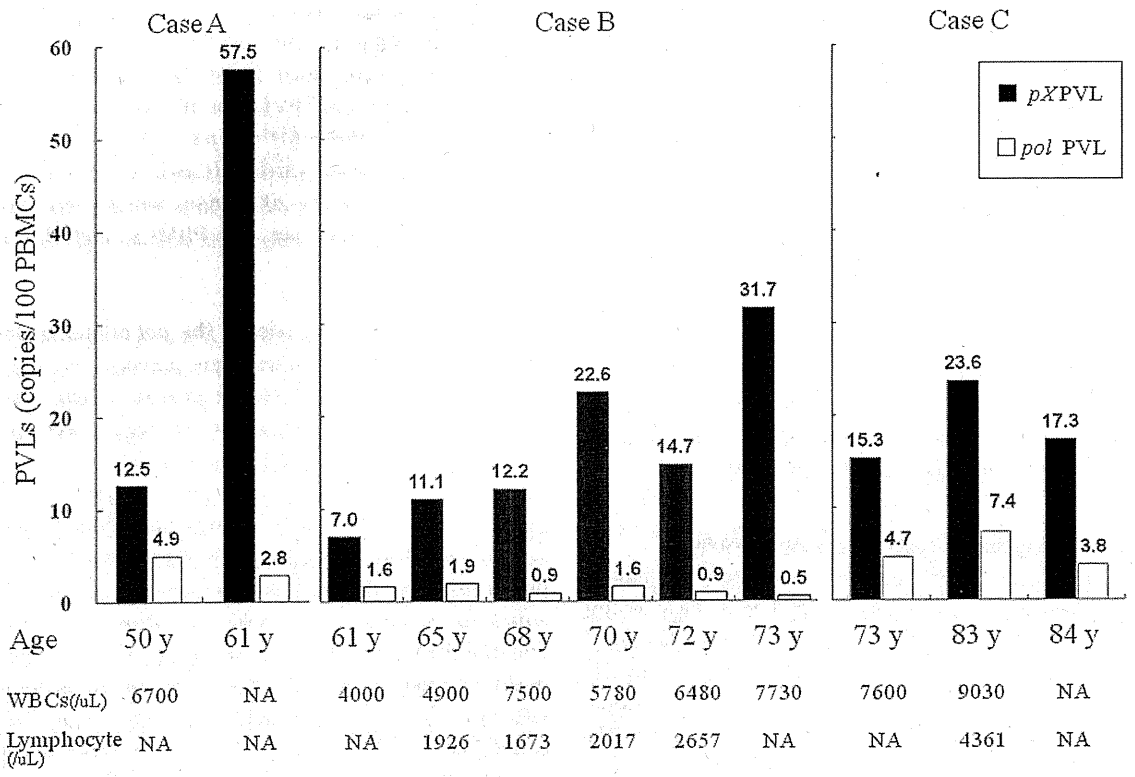

Figure 2. Proviral DNA loads for *pol* and *pX* regions at different ages of Cases A, B and C. WBCs: white blood cells; NA: not available.

symptoms suggesting ATL- and HTLV-1-associated diseases. The numbers of white blood cells and lymphocytes in their peripheral blood were within normal limits with no abnormal cells observed during the follow-up period. Cases A, B and C had high PVLs for the *pX* region, which were greater than 15 copies per 100 PBMCs at the most recent screens, when the cases were 61, 73 and 84 years old, respectively. PVLs for both the *pol* and *pX* regions were measured in previous time-sequential samples from these cases (Fig. 2). PVLs for the *pX* region in Cases A and B showed a marked increase during the 11- and 12-year follow-up, and those for the *pol* region showed either no change or decreased.

Sequencing and analysis for defective provirus in three cases

Long PCR to amplify the HTLV-1 provirus using primers for 5′ LTR and for the *pX* region was performed in the time-sequential samples from Cases A, B and C (Fig. 3). This long PCR amplifies the complete provirus and the Type 1 defective provirus with 5′ LTR conserved. In other words, Type 2 defective provirus, which does not conserve 5′LTR, is not amplified by this long PCR. If the subject had a complete proviral genome, the size of PCR product would be expected to be 7.7 kb. If the PCR products were smaller than 7.7 kb, they were judged to be derived from Type 1 defective provirus.

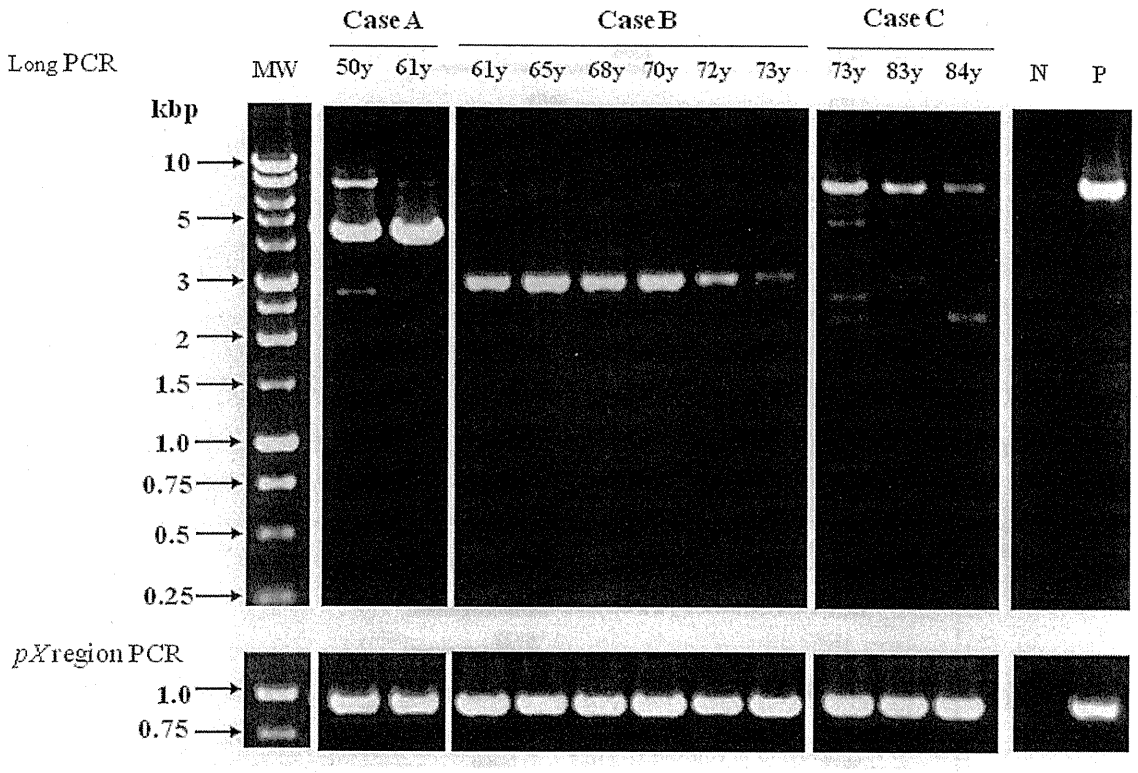

Figure 3. Detection of defective provirus by long polymerase chain reaction at different ages of Cases A, B and C. MW: molecular weight marker; N: human T-lymphotropic virus Type 1 (HTLV-1) negative subject; P: HTLV-1-positive cell line, ED-40515.

In Case A, a strong band of 4.5 kb and a weak band of 2.7 kb were detected in addition to a band of 7.7 kb at age of 50 years. When Case A was 61 years old, the strong 4.5 kb band increased its intensity. In contrast, the weak band of 2.7 kb was not detectable, and the band for the complete proviral genome decreased its intensity. The DNA sequence of the strong band of 4.5 kb showed that this band represented a Type 1 defective provirus with a 3.2-kb deficiency (positions 1203–4368, Fig. 4).

In Case B, a strong band of 2.9 kb was detected in addition to a weak band of 7.7 kb at age of 61 years. The DNA sequence of this 2.9 kb band showed that this band also represented a Type 1 defective provirus with 4.8 kb deficiency (positions 1173–5958, Fig. 4). When Case B was 73 years old, the intensity of the 2.9 kb band decreased markedly (Fig. 3). However, PVLs in Case B gradually increased as time passed (Fig. 2). Therefore, HTLV-1-infected cells harboring 2.9-kb Type 1 defective provirus were assumed not to be responsible for the increase of PVLs in Case B. In other words, HTLV-1-infected cells harboring provirus, which was not detected by long PCR used in our study, increased in number.

In Case C, several bands smaller in size than 7.7 kb, which might represent different Type 1 defective provirus, were detected. However, they were not consistently detectable at the ages of 73, 83 and 84. The 7.7-kb band of the complete proviral genome also decreased its intensity at the age of 84 years. The PCR product at age of 83 years was subcloned, and the DNA sequence was identified (Fig. 4). Thirteen Type 1 defective proviruses were detected in the 33 colonies derived from PCR products except for provirus with complete genome. Four of these were found to have insertions of nonviral sequences (clone cc-1,-3,-4 and -6, in Fig. 4).

Analysis of clonality of HTLV-1-infected cells by Southern blotting

To examine the clonal expansion of HTLV-1-infected cells, samples of genomic DNA (10 μg) from Cases A, B and C were analyzed by Southern blotting (Fig. 5). In Case A, a 17-kb band (a-1) was detected both at 50 and 61 years of age. The intensity of a-1 increased markedly at age 61. The increased intensity of clone a-1was consistent with the finding of increased PVLs for the *pX* region (Fig. 2) and with the increased intensity of the 4.5-kb band of Type 1 defective provirus by long PCR (Fig. 3). In addition, another weak band (a-2) was detected at age 61. Because the size of a-2 was ~7 kb, which was smaller than the size of complete HTLV-1 provirus (9 kb), a-2 was considered to be a clone with defective provirus, which was not detected by long PCR. In Case B, two clones (b-1 and b-2) were detected both at

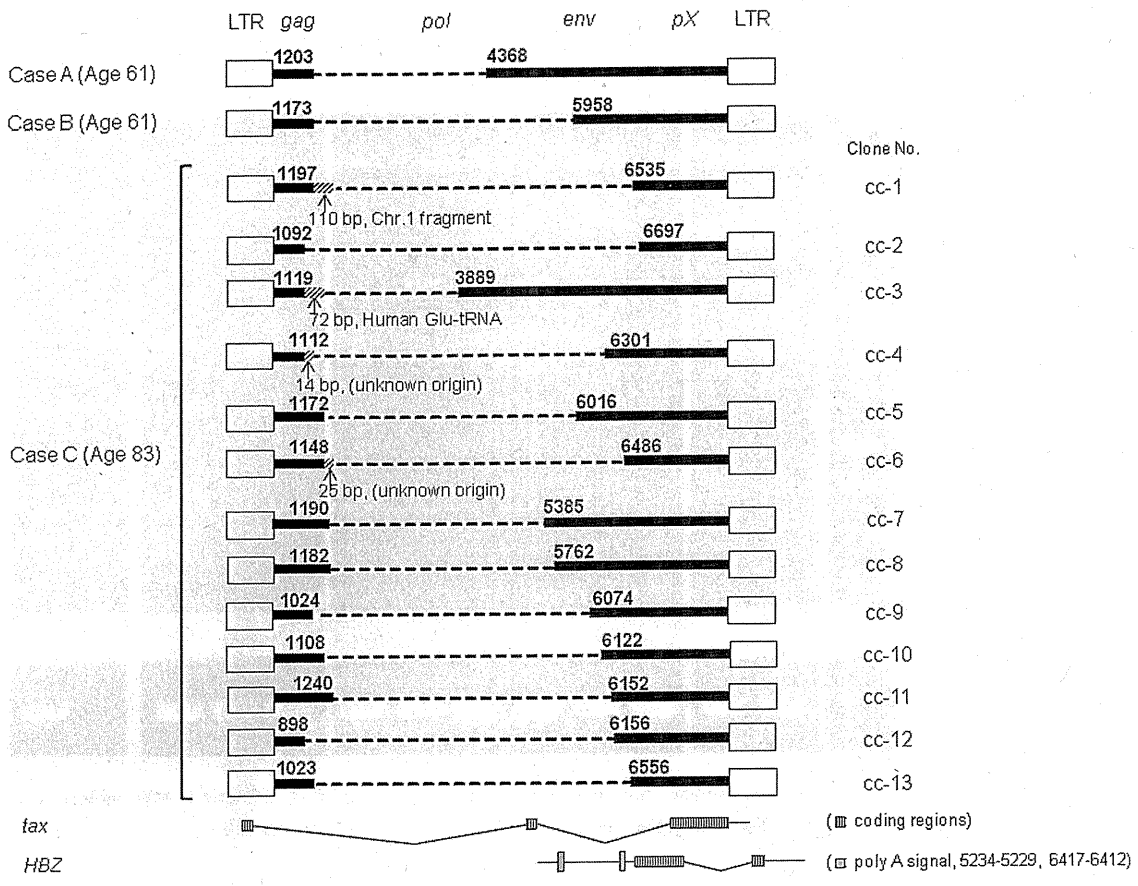

Figure 4. The schema of Type 1 defective provirus in Cases A, B and C. Dotted lines represent the defective regions of provirus. Splicing patterns of *tax* and *HBZ* genes are revealed. The nucleotide position numbers of human T-lymphotropic virus Type 1 (HTLV-1) provirus are same as those of Figure 1.

ages 61 and 70. The intensity of b-2 did not change during 9 years; however, that of b-1 increased at the age of 70. PVLs for the *pX* region increased (Fig. 2); however, the intensity of 2.9-kb Type 1 defective provirus by long PCR showed no change or decreased at age 70 (Fig. 3). Therefore, it was possible that clone b-2 represented the HTLV-1-infected cells with 2.9-kb Type 1 defective provirus detected by long PCR, and that another clone (b-1) of HTLV-1-infected cells with provirus, which was not detectable by long PCR, contributed to the increase of the PVLs in Case B. In Case C, one clone (c-1) was detected both at ages 73 and 84, and the other clone (c-2) was detected only at age 84. The intensity of c-1 was somewhat increased at the age of 84. The size of c-2 was ~7 kb and was considered to be a clone with defective provirus. However, clones c-1 and c-2 were not considered to be harboring Type 1 defective provirus because no band was observed to be increased in intensity at age 84 by long PCR (Fig. 3).

Discussion

To identify asymptomatic carriers, who have PBMCs harboring defective provirus with large deletions, PVLs of 208 asymptomatic HTLV-1 carriers were determined by real-time PCR using primers for the *pol* and *pX* regions. HTLV-1 *pX* region has been reported to be well conserved in the proviral genome.[14,16] Therefore, as expected, PVLs for the *pol* region were lower than those for the *pX* region. The carriers showing PVLs for the *pol* region, which were lower than those for the *pX* region, were considered to be candidates who have many PBMCs harboring defective provirus with large deletions of internal sequences. One hundred and eleven asymptomatic carriers showed relatively high PVLs (equal to or greater than 1.0 copy per 100 PBMCs). Seven showed low PVLs for the *pol* region (less than half of those for the *pX* region) among these 111 carriers. Four cases were excluded from further analysis because their low PVLs for the *pol* region were due to polymorphism of the proviral genome at the site of primer annealing. Three (Cases A, B and C) were considered as candidates for asymptomatic carriers, who have many HTLV-1-infected cells harboring defective provirus with large deletions. PVLs for the *pX* region increased in Cases A and B during follow-up for equal to or greater than 10 years. In contrast, PVLs for the *pol* region showed no change or decreased. These data suggested that the number

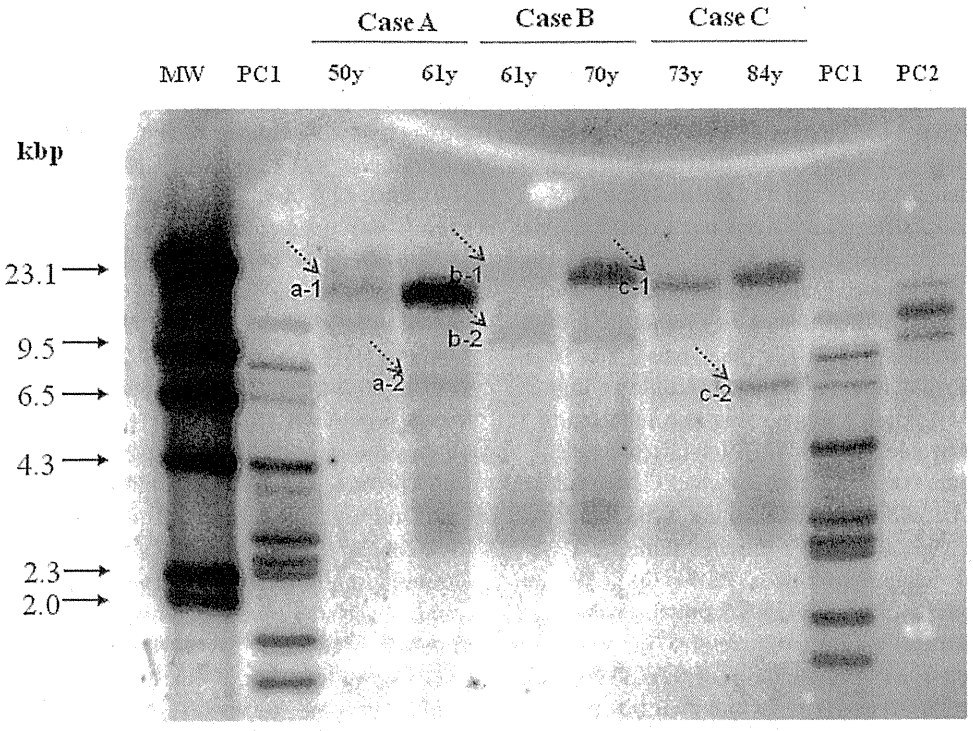

Figure 5. Southern blot analysis for human T-lymphotropic virus Type 1 (HTLV-1) provirus at different ages of Cases A, B and C. Arrows indicate predominant clones of HTLV-1-infected cells. PC1: DNA sample from HTLV-1-positive cell line, ST-1, which was digested with *Pst* I; PC2: DNA sample from HTLV-1-positive cell line, SO_4, which was digested with *Eco* RI; MW: molecular weight marker.

of HTLV-1-infected cells harboring defective provirus increased in Cases A and B.

Then, the defective provirus and the clonality of HTLV-1-infected cells were analyzed for the time-sequential samples from each subject. In Case A, a Type 1 defective provirus with a deletion of internal sequence of 3.2 kb was evident at the age of 50, and its intensity increased at age 61 (Fig. 3). Therefore, the increase of PVLs for the *pX* region, not for the *pol* region, was considered because of the clonal expansion of the HTLV-1-infected cells with this Type 1 defective provirus. Southern blot analysis showing the increased intensity of clone a-1 at age 61 supported this hypothesis. In Case B, a Type 1 defective provirus with the deletion of internal sequence of 4.8 kb was evident at age 61 (Fig. 3). The increase of PVLs for the *pX* region was not explained by the expansion of the HTLV-1-infected cells with this Type 1 defective provirus because the intensity of the PCR product for this defective provirus decreased at ages 72 and 73. Southern blot analysis showed two clones at the age of 61. Clone b-2 showed the same intensity at ages 61 and 70; however, clone b-1 increased in intensity at age 70. Therefore, the HTLV-1-infected cells harboring the Type 1 defective provirus in this case were more likely to belong to clone b-2. The increased PVLs at ages 70–73 were considered to be due to an increased number of HTLV-1-infected cells, which belonged to clone b-1. Clone b-1 was assumed to harbor the defective provirus because only a very weak band for complete provirus was detectable by long PCR in Case B. However, the defective provirus accounting for clone b-1 was not detectable by long PCR and could be a Type 2 defective provirus. Alternatively, a polymorphism of the DNA sequence in the site of primers of long PCR in 5′-LTR for clone b-1 may explain the absence of the band for defective provirus by long PCR. Therefore, it was considered that two major clones with defective provirus existed in Case B at age 61, and only clone b-1 survived as time passed. In Case C, several bands, which may have represented different Type 1 defective provirus, were detected by long PCR in addition to the band for the complete provirus at age 73. These defective proviruses were not consistently detectable at ages 73, 83 and 84. The intensity of the band for the HTLV-1-infected cells with complete provirus was also decreased as time passed. Therefore, maintenance of high PVLs at the age of 84 was not explained by these Type 1 defective proviruses alone. HTLV-1-infected cells with defective provirus, which was not detectable by long PCR in our study, might exist in Case C. In fact, Southern blot analysis showed increased intensity of clone c-1 and the appearance of new clone c-2 at age 84 (Fig. 5). The data from Cases A, B and C in our study suggested that HTLV-1-infected cells with certain types of defective provirus could be the predominant clones and persist for several years; however, the clones of HTLV-1-infected cells do not always survive for a long time in asymptomatic carriers.

Furukawa *et al.* reported that clonally proliferated cells infected with HTLV-1 were detected and were stable for from 4 months to 3 years in patients with HAM/TSP and their seropositive family members without showing any significant indication of ATL.[23] None of Cases A, B and C in our study showed any symptoms and data suggesting ATL- or HTLV-1-associated diseases, even at the end of the follow-up. Therefore, these carriers were judged not to have developed clinical ATL although they had high PVLs and clonal expansion of HTLV-1-infected cells with defective provirus. HTLV-1 Tax protein has been shown to promote the proliferation of infected cells.[13,24] On the other hand, Tax is also reported to be a good target for the host cellular immune response to HTLV-1.[25] HBZ protein was also reported to be important for the proliferation of HTLV-1-infected cells.[26–28] The proviral genome for *HBZ* gene, which is transcribed from 3′LTR, can be conserved even in the Type 2 defective provirus.[16,18] The Type 1 defective provirus found in Case A possessed internal deletion (positions 1203–4368). Theoretically, the expression of Tax and HBZ protein is not prevented by this internal deletion. Therefore, Tax and HBZ may have promoted the proliferation of HTLV-1-infected cells harboring this defective provirus although this proliferation might have been controlled by cytotoxic T-lymphocytes (CTL) through the recognition of Tax. At the same time, this defective provirus cannot express envelope and core proteins, which were also reported as the targets for CTL in HTLV-1 carriers.[29] Therefore, HTLV-1-infected cells harboring this defective provirus may be able to avoid attack from CTL more efficiently. In Case B, Type 1 defective provirus detected by long PCR possessed larger internal deletion (positions 1173–5958). Theoretically, the expression of Tax was prevented because of the deletion of the second exon of the *tax* gene in this defective provirus. It is not clear whether the loss of the expression of Tax protein was related to the decreased intensity of this clone at age 73. Theoretically, this Type 1 defective provirus was able to express HBZ protein because the provirus genome of *HBZ* gene was conserved. In Case C, 13 Type 1 defective proviruses were found at age 83. Twelve among these 13 clones (except clone cc-3 in Fig. 4) had large internal deletions, which theoretically prevent the expression of Tax. Moreover, 4 of 12 clones had the deletions, which theoretically prevent the expression of HBZ protein because of either the deficiencies of the coding regions of *HBZ* and/or deficiencies of two poly A signals (clone cc-1, −2, −6 and −13 in Fig. 4). These large deletions of defective provirus might account for clones not being consistently detectable during a long period in Case C.

In Cases B and C, the increase of PVLs in the time-sequential samples could not be explained by the existence of HTLV-1-infected cells with Type 1 defective provirus. The different clones of HTLV-1-infected cells with defective provirus, which was not detectable by the long-PCR used in our study, might exist in these cases. Clonal expansion of HTLV-1-infected cells with defective provirus, which does not express Tax protein and may not be recognized by the CTL, but which does promote the proliferation of HTLV-1-infected cells under the expression of HBZ protein, was possible. Indeed, HTLV-1-infected cells harboring Type 2 defective provirus were found more frequently in patients with ATL, suggesting a greater potential for leukemogenesis.[17,18]

In Case C, 4 of 13 Type 1 defective proviruses were found to have insertions of nonviral sequences (clone cc-1, −3, −4 and −6 in Fig. 4). Tamiya *et al.* also reported that insertion of a nonviral sequence (35 bp), which was derived from human proline transfer RNA, between the primer binding site and *env* region of HTLV-1 provirus in a patient with ATL.[16] They assumed that this nonviral sequence was inserted into the defective provirus during reverse transcription because human proline transfer RNA had the 16-bp homologous sequence with the 5′-region of HTLV-1. In our study, the DNA sequences of the inserted nonviral sequences in clone cc-1 and −3 were compared to the sequence of the 5′-region of HTLV-1. However, the homologous sequence was not found, and we could not clarify the mechanism of insertions of nonviral sequences in the defective provirus in Case C.

A major limitation of our study is that we were unable to identify genome sequences of Type 2 defective provirus, which possibly existed in Cases B and C, because of technical limitations. Further study to identify Type 2 defective provirus in asymptomatic carriers through improved methodology is necessary. In addition, the number of cases in which defective provirus was analyzed was small in our study. The analysis of more cases may clarify whether the HTLV-1-infected cells harboring the defective provirus have a growth advantage.

In our study, PVLs measured using primers for the *pol* region were less than those for the *pX* region in 208 asymptomatic HTLV-1 carriers. Analysis of seven carriers, who had relatively high PVLs for the *pX* region but much lower PVLs for the *pol* region, showed that they had HTLV-1-infected cells with polymorphism of proviral genome for the *pol* region or with defective provirus. All three asymptomatic HTLV-1 carriers, who had many HTLV-1-infected cells with defective provirus, showed high PVLs. The PVLs in two of the carriers increased markedly after a 10- to 12-year interval. This increase was considered to be due to the expansion of HTLV-1-infected cells with defective provirus. Accordingly, it is suggested that HTLV-1-infected cells with certain types of defective provirus can be predominant clones; however, not all predominant clones of HTLV-1-infected cells survive for a long time. Therefore, the detection of major clones of HTLV-1-infected cells may not always predict the development of ATL. Further study is necessary to clarify whether certain types of defective provirus are related to disease outcome such as ATL.

Acknowledgement

The authors thank Dr. M. Maeda (Kyoto University) for providing ED-40515(−) cell lines.